© MAY 2026 | IRE Journals | Volume 9 Issue 11 | ISSN: 2456-8880
DOI: https://doi.org/10.64388/IREV9I11-1718212

Production of Biodiesel from Pig and D (African Native Pear) Oil with Cow Bone Ash as The Heterogeneous Catalysts

OGBUEFI CHINWENDU MABEL[1], JOSEPH OKECHUKWU EZEUGO[2], IBIAM PRINCE AMAUCHE[3]

[1, 2, 3]*Deptartment Chemical Engineering, Faculty of Engineering, Chukwuemeka Odumegwu Ojukwu University Uli, Anamber State, Nigeria*

Abstract *- The present study was performed to optimize biodiesel yield of Lard oil and African pear oil using a heterogeneous calcium methoxide (Ca $(OCH_3)_2$) from cow bone calcinated at 900^0C as a catalyst for transesterification process in the biodiesel production from African pear flesh oil and Lard oil. Response surface methodology (RSM) with a 5-level-4-factor central composite design was applied to investigate the effect of experimental factors on the percentage of fatty acid methyl ester (FAME) conversion. The pig fat collected from quarter slaughter house was rendered by heating over a heating mantle at a temperature of 110^0C for 30 minutes to a liquid fat and was filtered to remove the residues from bones meat and fats that could not dissolve in the process of rendering. The African pear sample collected was softened with warm water and the potter separated from the flesh and oven-dried. The pear oil was then extracted from the dried pear potter by soxhlet method of extraction from 1,200g of the grinded pear potter using n-hexane as solvent. The solvent was removed by using rotary-evaporator under vacuum to get the pear oil. A quadratic model with an analysis of variance obtained from the RSM is suggested for the prediction of FAME conversion. A yield of 95.02wt% and 90.01% biodiesel was obtained for Lard and African pear flesh oil respectively at the optimized conditions after validation of the RSM model. The optimum conditions obtained from the RSM were 2.5wt% of catalyst concentration, 10:1methanol-to-oil molar ratio and 135 min of reaction time. Fuel properties were analyzed as per ASTM methods. Under these conditions, the properties of the produced biodiesel satisfied the standard requirement from the optimization result, kinetic and thermodynamic parameters were also analyzed. The positive values of Ea, ΔH indicate that this process is endothermic. The results are encouraging for the application of Ca $(OCH_3)_2$ from cow bone for environmentally friendly and sustainable biodiesel production.*

Keyword: *Production of Biodiesel, Pig Fat Oil, African Native Pear Oil, Cow Bone Ash, Catalysts*

I. INTRODUCTION

As a country, Nigeria is highly dependent on petroleum for its activities. Petroleum derived fuels have been the main source of energy worldwide. This source is finite and at the current rate of consumption coming from the global population explosion, it will run out in the near future. A viable alternative is biodiesel. An alternative fuel must be technically feasible, economically acceptable and immediately available (Meher, *et al.*, 2006). Biodiesel as an alternative fuel, it has many advantages. It is derived from a renewable domestic source, which relieves the dependence on importation of petroleum fuels. It is biodegradable and non-toxic. In comparison with petroleum fuels, biodiesel has a more favourable combustion emission profile, such as low carbon monoxide emissions, particulate matter and unburnt hydrocarbons. Carbon dioxide produced by the combustion of biodiesel can be recycled through photosynthesis, thereby minimizing the greenhouse effect (Rao, *et al.*, 2008).

So far, this alternative fuel has been successfully produced by transesterification of vegetable oils and animal fats using homogeneous basic catalysts (mainly sodium or potassium hydroxide dissolved in methanol). Traditional homogeneous catalysts (basic or acidic) have advantages, including high activity (complete conversion within 1 hour) and mild reaction conditions (from 40 to 65 °C and atmospheric pressure). However, the use of homogeneous catalysts leads to soap production and it also leads to lower biodiesel yield and increases the difficulty to separate biodiesel from glycerol which is a co-product (, et al; 2016..Beyond certain catalysis concentration, soap formation complicate biodiesel separation from glycerol fraction increases the biodiesel viscosity and decreased the FAME yield (Bhatti H. N., et al., 2008) (Hoque &Chuna Yi, 2011)..Moreover, the method of

removing the catalyst after the reaction is technically difficult and a large amount of waste water is produced to separate and clean the products, which increases the overall cost of the process.

The total costs of biodiesel production on the basis of homogeneous catalysis are therefore not yet sufficiently competitive compared to the costs of diesel production from petroleum. An alternative is the development of heterogeneous catalysts that could eliminate the additional operating costs in connection with the abovementioned phases of separation and purification. Thus, the costs of process equipment are generally lower compared to a homogeneously catalyzed process. In this study the heterogeneously catalyzed production process of biodiesel is applicable. Later, sensitivity analysis and optimization are performed to determine the effect of operating parameters and to find optimal parameters. So much oil from both plants and animal sources has been used in the past in the production of biodiesel. In this research pig oil (lard) and African pear flesh oil will be used as the raw materials and the cow bone ash as the source of heterogeneous catalysts.

Increasing environmental concern, diminishing petroleum reserves, and agriculture-based economy of our country are the driving forces to promote biodiesel as an alternative fuel. Non-biodegradable and toxic nature of petroleum fuel and combustion emission profile, such as high emission of carbon monoxide, particulate matter and unburned hydrocarbons produced by combustion of petroleum diesel cannot be recycled, thereby increasing the greenhouse gas effect on the ecosystem thus, the reasons for exploring the use of animal fats and plant oil as an alternative to fossil fuel (Rao, *et al.*, 2008). Such oils usually contain some water and free fatty acids (FFAs) that will form soap when homogeneous base catalysts are used. On the other hand, homogenous acid catalysts are corrosive to equipment. Solid heterogeneous catalysts are used to overcome these problems, because they are noncorrosive, non-toxic, and easily-separated for recycling. Reusability of heterogeneous catalysts makes continuous fixed-bed operation possible. Such continuous process can minimize product separation and purification costs, make it economically viable to compete with commercial petroleum-based diesel fuel.

This research will be a good source of income both to the country and to individuals when logically implemented. The rate of unemployment in the country will reduce drastically when people engage into the extraction and production process as the job they do. Also, we will have as fuel a better source of energy that is technically acceptable, economically competitive, environmentally acceptable, cost effective and easily available.

II. MATERIALS AND METHODS

2.1 Materials

Pork fat, African pear oil, cow bone, methanol, beakers, heating flask, hotplate, separation funnel, sieves, muffle furnace, oven,

2.2 Experimental Methods

2.2.1 Collection of Pig Fat Sample and Extraction of Lard Oil

Pig fat was collected from quarter slaughter house in Awka South L.G.A in Anambra state, and was rendered by heating over a heating mantle at a temperature of 110^{o}C for 30 minutes to a liquid fat and was filtered to remove the residues from bones, meat and fats that could not dissolve in the process of rendering.

2.2.2 Extraction of Oil from Pear Flesh Oil

The African pear sample was collected softened with warm water and the potter separated from the flesh and oven-dried. Pear oil was extracted from the dried pear potter by Soxhlet method of extraction from 1,200g of the grinded pear potter using n-hexane as solvent. The solvent was removed by using rotary-evaporator under vacuum to get the pear oil. The weight of the pear oil extracted was taken to determine the oil yield.

$$\%\ Oil\ extracted = \frac{weight\ of\ oil\ extracted \times 100}{\text{Weight of sample used}} \quad (2.1)$$

2.2.3 Pre-treatment of the Oil Extract

A pre-treatment procedure was performed on the oil extract due to its high free fatty acid (FFA) content of 5.95 mg/KOH/g for lard oil and 28.25 mg/KOH/g. The FFA was reduced below 1.0% using methanol and concentrated sulphuric acid as catalyst prior to transesterification reaction.

Eighty-seven millilitres (87 ml) of the oil were weighed into a 500 ml flat bottomed flask, 12 ml of methanol and 1% H_2SO_4 were added. The mixture was agitated at a high speed of 450 rpm and temperature of

60°C using magnetic stirrer with a reaction time of 120 min.

2.2.4 Dehydration of Oil Extract

Lard/pear oil was filtered under vacuum, after dehydrated using anhydrous sodium sulphate (left over night) and finally again filtered under vacuum. The pork lard/pear oil was first heated at 100 ºC to eliminate residual water and after cooled to near the reaction temperature before transesterification process.

2.2.5 Calcination of Cow Bone

Dry and grinded cow bone was calcinated in a muffle furnace at a temperature of 850ºC for 2 hours. The calcinated cow bone ash was cooled crushed further and sieved to obtain fine powder which was used as a catalyst for the reaction.

2.2.6 Transesterification Procedure

A batch reactor of 500 ml capacity equipped with a reflux condenser and magnetic Stirrer was charged with the desired amount of oil (50 ml) heated to 65°C at a particular speed of agitation. A measured amount of catalyst (cow bone ash) was then thoroughly mixed in known quantity of methanol to give calcium methoxide. The calcium methoxide was added to the reactor and the reaction timed immediately after the addition of the calcium methoxide.

It was transferred into separating funnel and allowed to settle for an hour. Two distinct layers were observed; a thick brown layer (glycerol) at the bottom and a yellowish colour layer constituting the upper layer (biodiesel).

FAME layer (Biodiesel) with methanol was separated from glycerol and heated slightly to remove any residual water in it. The percentage yield was calculated using equation (2.2).

$$\%\, Yield = \frac{Weight\ of\ Fatty\ Acid\ Methyl\ Ester \times 100}{\text{Weight of oil used}} \quad ----------(2.2)$$

The transesterification was carried out at optimum rotation speed of 250 rpm based on literature data to achieve maximum conversion.

The reaction parameters were chosen as follows: temperature ranged from 45°C to 75°C, mass ratio of catalyst to oil from 0.5% to 1.5%, time from 45 min to 75 min, molar ratio of methanol to oil from 2:1 to 6:1. The procedures above were used for each experiment executed at different parameters using the experimental design matrix as designed for this work and attached in the index at the back of this work.

2.2.7 Physical and Chemical Characterization of the Raw oil and Biodiesel

The extracted oil was characterized for various analysis such as, Specific gravity, Density, Viscosity, Acid value, free fatty acid value, Saponification value, Iodine value, moisture content, Refractive index, sulphur content, pour point, flash point, cloud point.

2.2.8 Physical and Chemical Characterization of the Raw oil and Biodiesel

2g of the oil was measured and poured in a beaker. A neutral solvent (a mixture of petroleum ether and ethanol) was prepared and 50ml of it was taken and poured into the beaker containing the oil sample. The mixture was stirred vigorously for 30minutes. 0.4g of sodium hydroxide (NaOH) pellet was measured and placed in a separate beaker and 0.1M NaOH was prepared, 1ml of phenolphthalein indicator was added to the sample and was titrated against 0.1M NaOH till the colour change observed turned pink and persisted for 15minutes.

$$AV = \frac{Titre \times 5.61}{Wt\ of\ oil\ sampled\ used} \quad ----------(2.3)$$

$$FFA = \frac{AV}{2} \quad ----------(2.4)$$

2.2.9 Determination of Saponification Value

The alcoholic KOH was freshly prepared by dissolving KOH pellet in ethanol. 2g of oil was measured and poured into a conical flask. 25ml of the alcoholic KOH was added to it, a blank was used. The sample was well covered and placed in a steam water bath for 30minutes shaking it periodically, 1ml of phenolphthalein was added to the mixture and titrated against 0.5M HCl to get the end point (*Ibiam et al.*, 2022).

$$SV = \frac{(b-a) \times 28.05}{wt\ of\ sample} \quad ----------(2.5)$$

Where; b= volume of 0.5M HCl used in blank titration;

a=volume of 0.5M HCl used in titration with the oil;

2.2.10 Determination of Iodine value

© MAY 2026 | IRE Journals | Volume 9 Issue 11 | ISSN: 2456-8880
DOI: https://doi.org/10.64388/IREV9I11-1718212

0.3g of the raw oil/biodiesel was weighed into a small beaker, 10ml of carbon tetrachloride was added into the oil in the beaker to dissolve the oil. 20ml of Wijis solution was added and covered and allowed to stand in the dark for 30mins. 15ml of potassium iodide solution (10%) was added and 100ml of distilled water mixed with it and titrated against 0.1M sodium thiosulphate solution using starch as an indicator. A blank solution was also done at the same time with the samples.

$$Iodine\ value = \frac{(b-a) \times 1.269}{Weight\ of\ sample} \quad ---------- (2.6)$$

2.2.11 Determination of Moisture Content

In other to determine the moisture content in the oil (%), 2g of oil was weighed in a crucible, the weight of the crucible and oil was taken and was put inside an oven for 3hours at a temperature of 105ºC. After every 1hour, the sample was cooled and weighed until the weight before and after was approximately equal (*Ibiam et al.*, 2022).

$$\frac{W_2 - W_3 \times 100}{W_2 - W_1} \quad ---------- (2.7)$$

Where: W_1 – weight of empty crucible
W_2 – weight of crucible + sample before oven drying
W_3 – weight of crucible + sample after oven-drying

2.2.12 Determination of Specific Gravity/Density (ASTM D1298) by Hydrometer Method

A clean dry empty 50ml density bottle was weighed and the mass recorded as M, it is then filled up with distilled water and subsequently with the samples. The mass of the bottle and water is taken and recorded as M1 and that of oil/ biodiesel as M2 respectively hence, the specific gravity is evaluated. This procedure is used to determine the specific gravity of the sample.

$$\frac{W_2 - W_1 1 \times 100}{W_3 - W_1} \quad ---------- (2.8)$$

Where: W_1 – weight of empty density bottle
W_2 – weight of density bottle + sample
W_3 – weight of density bottle + water

2.2.13 Determination of Kinematic Viscosity (ASTM D 445)

An Osward Chamber viscometer is inserted into oil/biodiesel bath with a set temperature and left for 30minutes to stand and take the viscosity reading on the viscometer read-out. The procedure is repeated a number of times and the average value are taken to give the kinematic viscosity at two different temperature of 40^0 C and 100^0 C

2.2.14 Determination of Flash Point: ASTM D 93

A sample of the biodiesel is heated in a close vessel and ignited. When the sample burns, the temperature is recorded, the pensky-martens cup tester measures the lowest temperature at which application of the test flame causes the vapour above the sample to ignite. The biodiesel is placed in a cup in such quantity as to just touch the prescribed mark on the interior of the cup. The cover is then fitted onto the position on the cup and Bunsen burner is used to supply heat to the apparatus at a rate of about 5^0C per minute. During heating, the oil is constantly stirred. As the oil approaches its flashing, the injector burner is lighted and injected into the oil container after every 12 second intervals until a distinct flash is observed within the container. The temperature at which the flash occurred is then recorded, it is repeated three times and the average taken.

2.2.15 Determination of Cloud Point and Pour Point (ASTM D 2500, ASTM D 97))

A sample of the biodiesel is placed in a test jar to a mark and then placed inside a cooling bath. The temperature at the bottom of the test jar that is the temperature at which the biodiesel starts to form cloud is taken as the cloud point.

A sample of the biodiesel that is kept in the freezer to about 5ºC then placed in a heating mantle to melt. The temperature at the bottom of the test jar that is the temperature at which the biodiesel starts to pour is taken as the pour point (*Ibiam et al.*, 2022).

2.2.16 Molecular Weight Determination

The molecular weight of the oil was calculated as (Xu *et.al.,*2006)

$$\text{MW} = {}^{168300}/_{SV-AV} \quad ---------- (2.9)$$

Where: MW-molecular weight of oil
SV- Saponification value of oil
AV- acid value of oil

2.2.17 FTIR

A pure liquid sample of the oil/biodiesel was placed between two disks of pure KBr and the resulting 'sandwich' placed directly in the sample holder of the spectrometer (IR Bulk Scientific, model 530).

Excellent spectra were obtained in a matter of a few minutes with minimum expense.

2.2.18 GC Analysis

Analysis of biodiesel was performed through a GC-FID (Bulk scientific 910 model). Sample injection took place at the oven temperature of 50°C and was maintained at 50^0C for I min, the temperature was increased up to 325^0C at the heating rate of 10^0 C min-1 and hold at 325^0C for 2 min. The GC-FID interface temperature was set to 250^0C and helium was used as a carrier gas.

2.2.19 Procedure for BET Analysis

The bone sample was Properly weighed into the sample cell. The filled sample cell bulb was insert into the heating mantle. The clamp was placed around the mantle so that the sample cell is held firm. The sample cell stem was inserted into the sample preparation station. The knurled ring was tightened by turning it clockwise to secure the sample cell in the preparation station.

After the sample cell(s) secured in the preparation station, out gassing was initiated by entering the control panel menu on the instrument, the outgassing temperature was set to 300°Cand the system instructed to start degassing and the heater switched on. When the sample has out gassed for 3hour's the heating mantle was turned off, the heating mantle and the sample cell was allowed to cool. Once the heating mantle was cooled, the out-gas station was unloaded and the samples removed. The sample cell was reweighed to determine the post out gas sample weight.

2.2.20 Sample Analysis

Nova 4200e Made in USA was used for the BET analysis. The dewater was filled to the internal upper mark with liquid nitrogen, the sample cell containing an out gassed and weighed sample was placed into the analysis station to be used for analysis. All the fields/selections on the start analysis ''Sample'' menu was completed. Also point selection and tagging on the start Analysis ''Points'' menu was completed. The fields on the start Analysis ''Equilibrium'' menu was completed. Field defaults can be used for BET measurements! When all fields are completed on the start Analysis Menu, the ''Start'' button was clicked to begin the analysis.

2.2.21 XRF Analysis

The first step taken was to check the energy calibration to ensure that peak energies are accurately tied to specific elements. Energy adjustment is performed using a Thermos Noran copper (Cu) calibration standard. This procedure is run every day before any analysis is performed. The energy adjustment involves measuring the Cu K" line (8041), and then determining the difference between the measured peak energy value and the ideal value and if any adjustments are required, the instrument software performs it automatically. Filtered samples were removed from cold storage and were loaded into the sample cups. Sample information was entered into the instrument logbook. The filters (in their sample cups) were loaded into the XRF sample tray in the same order as they were written into the instrument logbook. The instrument was then prepared for analysis by entering each filter aliquot number into the Method Tray List within the Win Trace software. The PM filter deposit analysis was then initiated. After the filters were loaded into the sample cups and loaded into the sample tray, a Method Tray List was created in Acquisition Manager within the Win Trace software. The Method Tray List will allow for automated quantitative analysis in conjunction with a Method File. The Method Tray List was created by entering the first sample identification and choosing the Method File from the directory. After the Method File was opened by Acquisition Manager and the sample position was verified in the tray as being correct, then was the next sample on the next line entered. The program automatically filled in the Method File specified for the previous sample. After the Method Tray List was set up, the spectrum icon on the toolbar was clicked to start the acquisition. The chamber lid was latched and the "X-RAYS ON" warning light was illuminated and the vacuum pump was clicked on. After a 300-second warm up, acquisition was began starting with the lowest power condition. After all the spectra have all been acquired (they were saved in the respective Method File), Method Explorer processed the spectrums and displayed the analytical results in a specific format. The instrumental analysis report detailed the analyte, concentration, uncertainty, peak counts per second (cps), and background cps. To obtain the analytical results of the unknowns, we went to Method Explorer and open the respective Method File. Under sample lists, the samples needed were identified, and then clicked on the analysis report item to obtain the results in an rtf format. The report was saved onto the hard drive and also the hard copy printed out.

© MAY 2026 | IRE Journals | Volume 9 Issue 11 | ISSN: 2456-8880
DOI: https://doi.org/10.64388/IREV9I11-1718212

2.2.22 Scanning Electron Microscope (SEM)

The scanning electron microscopy (SEM) was performed to examine the physical structure change of samples using SEM model Phenom ProX, by phenom World Einhoven, The Netherlands. Sample was placed on double adhesive which was on a sample stub, was coated sputter coater by quorum technologies model Q150R, with 5nm of gold. Thereafter it was taken to the chamber of SEM machine where it was viewed via NaVCaM for focusing and little adjustment, it was then transferred to SEM mode, was focused and brightness contrasting was automatically adjusted, afterward the morphologies of different magnification was store in a USB stick.

2.2.23 XRD

The analyzed material was finely ground, homogenized, and average bulk composition is determined. The powdered sample was then prepared using the sample preparation block and compressed in the flat sample holder to create a flat, smooth surface that was later mounted on the sample stage in the XRD cabinet.

The sample was analysed using the reflection-transmission spinner stage using the Theta-Theta settings. Two-Theta starting position was 4 degrees and ends at 75 degrees with a two-theta step of 0.026261at 8.67 seconds per step. Tube current was 40mA and the tension was 45VA. A Programmable Divergent Slit was used with a 5mm Width Mask and the Gonio Scan was used. The intensity of diffracted X-rays is continuously recorded as the sample and detector rotate through their respective angles. A peak in intensity occurs when the mineral contains lattice planes with d-spacings appropriate to diffract X-rays at that value of θ. Although each peak consists of two separate reflections ($K\alpha_1$ and $K\alpha_2$), at small values of 2θ the peak locations overlap with $K\alpha_2$ appearing as a hump on the side of $K\alpha_1$. Greater separation occurs at higher values of θ. Typically these combined peaks are treated as one. The 2λ position of the diffraction peak is typically measured as the center of the peak at 80% peak height.

Results are commonly presented as peak positions at 2θ and X-ray counts (intensity) in the form of a table or an x-y plot (shown above). Intensity (*I*) is either reported as peak height intensity, that intensity above background, or as integrated intensity, the area under the peak. The relative intensity is recorded as the ratio of the peak intensity to that of the most intense peak (*relative intensity* = $I/I_1 \times 100$).

2.2.24 TGA Procedure:

Part 1:

The log MUST be filled out. It is recommended that this be done before beginning a measurement so as not to forget.

Part 2:

Please remember to check that the nitrogen gas is on and that it is connected to the instrument in the "balance" port. If the tank regulator reads below 400psi, please contact the SIT immediately. Do not attempt to change the tank unless approved to do so.

Part 3:

Open up "Pyris" manager. Select the TGA button at the top of the screen. Click only once. The software is slow and if you double click it will attempt to open twice.

When the software is open there will be two dialogs within the application (see figure) One is the instrument viewer and the other is the method editor. At the right is a column of icons that are used to send direct commands to the instrument. There are diagrams at the end of this document that show the commands. Terms in bold can be found in the diagrams. Select the <cool furnace> icon if the furnace is not already in that position.

Part 4:

Using the tweezers supplied with the TGA, load a clean empty crucible with the wire basket (stirrup) onto the hang-down wire. This must be done VERY carefully. Do not attempt until after a few practices runs with the SIT. The hang down wire is connected to the microbalance at the top of the instrument and is very expensive to fix or replace. Do not pull on the hang-down wire as it may be broken off from the arm on the balance mechanism.

After the crucible has been installed, select the <raise furnace> icon. The furnace will move into position and raise up over the crucible. When the furnace is in position select the <zero balance> icon. You will need to wait a few minutes to allow the crucible to stabilize and you may zero the balance repeatedly until it stabilizes.

When the balance has been satisfactorily zeroed, select the <cool furnace> icon to move the furnace out of the way. Put the sample stage in position under the crucible and hang down wire and carefully remove the crucible by lifting the wire basket from the hang down wire. Put your sample in the crucible and carefully reinstall the crucible and wire basket on the hang-down wire. Select the <raise furnace> icon and wait for the crucible with sample to stabilize. This may take up to 10 minutes. Also, if your sample has a lot of moisture, it may take more time. While the sample stabilizes go to the method editor and edit as needed. (Before running the measurement be sure to select the <measure sample> icon.

The value will automatically be recorded in the method editor; see below.)

Part 5:

In Method Editor, input information about your sample. Select browse to name and save your data file. Select the program tab and program as follows:

Starting temperature
First temperature scan
First isothermal
Second temperature scan
Repeat as necessary.

Maximum operating temperature is 1200 C, max heat up rate 20 C. The furnace does tend to overheat so this should be taken into consideration. A slower heating rate may be better. When you are satisfied with your method, if you have not done so already, save your method. Please be careful not to overwrite someone else's method. At this time weigh your sample using the <weigh sample> icon. Select the start icon.

Part 6:

When your measurement is complete you may put the furnace in the cool position and remove your crucible. If you need to run another sample the furnace will cool down faster in the raised position. Please keep your crucibles with you and do not leave crucibles or samples on or around the TGA workspace.

PerkinElmer
TGA 4000
Made in Netherlands

2.2.25 Oxidative stability Procedure

Methods of Oxygen Absorption (RapidOxy): was used for the oxidative stability. The RapidOxy method consists of an accelerated oxidation process by increasing the pressure of oxygen and temperature, allowing us to determine the oxidative stability of the samples. It was carried out in oxygen pump device and the pressure drop was usually measured as a function of time. The samples were subjected to a pressure with pure oxygen of up to 700 kPa, while raising its temperature to 200 ° C. The temperature was maintained constant, while the pressure is measured continuously until a definite drop in pressure was detected.

2.2.26 Experimental Design

A five-level four-factor Central Composite Design CCD was employed in this study to examine the effect of independent variables such as temperature *A*, time *B*, catalyst concentration *C* and methanol / oil ratio *D* on the FAME content. The experimental values used for the employed levels are shown in Table 2.1 for both pig fat oil and African pear oil. The model was explained with 30 experimental runs $2^k + 2^k +$ where, *k* was the number of factors, and m is number replicated center points sixteen factorial points 2^k, eight axial points $2k$, and six replicated center Points $m = 6$. The Design Expert TM, Version 6.0 of Stat-Ease Inc. USA software was used for regression analysis on the data obtained. Statistical analysis of the model was performed to evaluate the analysis of variance ANOVA.

Once the experimental data obtained was fitted with a second-order model in order to correlate the response variable to the independent variable. The general form of second order polynomial equation:

$$Y = b0 + \Sigma^{k}_{i=1} b_i x_i + \Sigma^{k}_{i=1} b_i x_i^2 + \Sigma^{k}_{i=1} + \Sigma^{k}_{i=j} b_{ij} x_i x_j + e \quad (2.10)$$

where, *Y* is response FAME content, *b*0, *bi*, *bii* and *bij* are the regression coefficients obtained for constant, linear, quadratic and interaction terms, respectively. *Xi* and *xj* are independent variables, whereas *i* and *j* are the linear and quadratic coefficients, respectively, *b* is the regression coefficient, *k* is the number of factors studied and optimized in the experiment and *e* is random error.

2.2.27 Kinetics and thermodynamic studies

To better comprehend the nature of the process, it is essential to study the kinetics of the transesterification process. The transfer of the solute between the two phases takes place at a particular rate and it is necessary to investigate this rate. Moreover, the selection of the best condition can be achieved by altering the contact time. Kinetic study of the transesterification process of the lard oil and African pear oil would be performed on optimum process parameters of the system. The commonly used model

to discover the kinetics of transesterification is the general rate equation.

The biodiesel production yield from Lard oil and African pear oil would be found using Equation (2.11).

$dY/dt = kY^n$ ----------(2.11)

where, Y is the biodiesel yield (%); t is the time of transesterification (min); k is the rate constant (min^{-1}) and n is the order number. The term dY/dt having a positive sign shows that the percentage of biodiesel produced increases with time. The application of the differential method will show the plot of ln (dY/dt) vs ln Y to be linear. The order of the reaction will be determined from the slopes of the straight lines.

2.2.27.1 Activation energy

For a unit operation, it is crucial to have a chemical system with potential components for which activation energy is a must. A considerable number of molecules having translational energy that is bigger than the activation energy is required for the transesterification process to be carried out at a reasonable rate. Activation energy is the minimum energy required to begin a transesterification process which is normally denoted by Ea. The activation energy for the transesterification process can be determined from the rate constants.

Equation (2.12) shows the association between the rate constant and transesterification temperature as described by Arrhenius.

$k = Ae^{-Ea/RT}$ ---------- (2.12)

where, k is the reaction rate constant (min^{-1}); A is the Arrhenius constant (s^{-1}); Ea is the activation energy (kJ mol^{-1}); R is the universal gas constant t (J mol^{-1} K^{-1}) and T is the absolute temperature (K). A plot of ln k versus 1/T yields a straight line with the slope representing the activation energy of transesterification (–Ea/R) and an intercept as the Arrhenius constant (ln A).

2.2.27.2 Thermodynamic parameters

The transesterification of oil using methanol as the solvent involves thermodynamic parameters (ΔH, ΔS and ΔG) which will be estimated using Equations (2.13) and (2.14).

$K^* = YT/YU$ ----------(2.13)

$\ln K^* = -\Delta G/RT = -\Delta H/RT + \Delta S/R$ ----------(2.14)

The slope of a straight line given by the plot of lnYT versus 1/T (Figure 2) represents the enthalpy change in extraction (–ΔH). Thus, the enthalpy change was calculated to be

ΔH¼ = 0.1140 kJ $mol^{-1}$for extraction.

Table 2.1: Study range of values

Factor	Low level	High level	axial(-α)	axial(+ α)	Center point
A	40	60	30	70	50
B	90	180	45	225	135
C	2.0	3.0	1.5	3.5	2.5
D	8	12	6	14	10

Table 2.2: Design matrix for Transesterification of African Pear oil

Std	Runs	Tempt	Time	Catalyst	Methanol	% Yield
13	1	40	90	3	12	
26	2	50	135	2.5	10	
8	3	60	180	3	8	
28	4	50	135	2.5	10	
3	5	40	180	2	8	
21	6	50	135	1.792893	10	
30	7	50	135	2.5	10	
6	8	60	90	3	8	
17	9	35.85786	135	2.5	10	
22	10	50	135	3.207107	10	
5	11	40	90	3	8	

15	12	40	180	3	12
19	13	50	71.36039	2.5	10
7	14	40	180	3	8
23	15	50	135	2.5	7.171573
18	16	64.14214	135	2.5	10
27	17	50	135	2.5	10
9	18	40	90	2	12
4	19	60	180	2	8
10	20	60	90	2	12
29	21	50	135	2.5	10
12	22	60	180	2	12
14	23	60	90	3	12
20	24	50	198.6396	2.5	10
11	25	40	180	2	12
24	26	50	135	2.5	12.82843
2	27	60	90	2	8
1	28	40	90	2	8
25	29	50	135	2.5	10
16	30	60	180	3	12

Table 2.3: Design matrix for Transesterification of Lard oil

Std	Runs	Tempt	Time	Catalyst	Methanol	% Yield
13	1	40	90	3	12	
26	2	50	135	2.5	10	
8	3	60	180	3	8	
28	4	50	135	2.5	10	
3	5	40	180	2	8	
21	6	50	135	1.792893	10	
30	7	50	135	2.5	10	
6	8	60	90	3	8	
17	9	35.85786	135	2.5	10	
22	10	50	135	3.207107	10	
5	11	40	90	3	8	
15	12	40	180	3	12	
19	13	50	71.36039	2.5	10	
7	14	40	180	3	8	
23	15	50	135	2.5	7.171573	
18	16	64.14214	135	2.5	10	
27	17	50	135	2.5	10	
9	18	40	90	2	12	
4	19	60	180	2	8	
10	20	60	90	2	12	
29	21	50	135	2.5	10	
12	22	60	180	2	12	
14	23	60	90	3	12	
20	24	50	198.6396	2.5	10	

11	25	40	180	2	12
24	26	50	135	2.5	12.82843
2	27	60	90	2	8
1	28	40	90	2	8
25	29	50	135	2.5	10
16	30	60	180	3	12

III. RESULTS AND DISCUSSION

3.1 Characterization of Oil from Pig Fat and African Pear

3.1.1 Physiochemical properties of the oils

From the table 3.1 below it showed that the Pig fat (Lard oil) and the African pear (Ube) oil meet with the ASTMD6751 on iodine value, specific gravity, density, and viscosity. Both the African pear flesh and pig fat oils contain high acid/free fatty acid values of 5.21/2.605 mg/KOH/g and 2.82/1.41 mg/KOH/g respectively. These high values will require the need for pre-treatment step to be carried out on the raw oils before the transesterification step to avoid the catalyst used in the conversion reaction from reacting with the excess FFA to form soap but, this was taken care of by the heterogeneous catalyst used in the direct transesterification process without necessarily undergoing pre-treatment step. Soap formation is undesirable as it lowers the yield of biodiesel and inhibits separation of biodiesel from glycerol (Widyan and Shyoukh, 2002). In addition, excess FFA binds with catalyst and consequently leads to more consumption of the catalyst, which implies a high cost of production (Soriano *et al.*, 2009). The physicochemical properties of the raw oils compared favourably with those of some other none edible oils such as *Pongamia pinnata* (Agarwal and Garima, 2011), *Jatropha curcas* (Adebayo *et al*., 2011), *Madhuca indica* (Azam *et al.*, 2005).

Table 3.1: Physicochemical analysis on the raw African pear and lard oils compared with ASTMD6751

Parameter	ASTM D6751	Lard oil	African Pear oil
Moisture(%)	0.05 max	9.5	8.54
Acid value (mgKOH/g)	0 – 0.50	2.51	1.25
FFA(mgKOH/g)	0 – 0.5	4.51	2.44
Iodine value (gI_2/100g)	< 125	58.79	59.56
Saponification Value (mgKOH/g)	-	289.74	584.66
Peroxide value (MEq/kg)	-	17.2	15.0
Specific gravity	0.86 – 0.90	0.9211	0.9021
Density(g/ml)	0.888 minimum	0.8642	0.8978
Refractive index	-	1.4634	1.4638
Viscosity@ 40 (pa.s)	1.9 – 6.0	2.42050	2.14301
Viscosity@100 (pa.s)	-	2.3929	1.5271
Flash point(^{0}C)	130 minimum	-	-
Fire point(^{0}C)	-	-	-
Cloud point(^{0}C)	-3 to 12	-	-
Pour point(^{0}C)	-15 to 10	-	-
Cetane number	47 minimum	-	-
Sulphure	0.05 max	-	-
Sulphated Ash	0.02 max	-	-
Carbon Residue	0.05 max	-	-

3.1.2 Fatty acid profile of the oil

The fatty acid composition of African pear flesh and pig fat oils is given in Table 3.2. African pear flesh oil comprises 72.19% saturated acids (palmitic, lauric, myristic and stearic) and 27.77% unsaturated acids (oleic, linoleic and eicosatetraenoic). The dominant monosaturated fatty acid of the oil was myristic, which accounted for 24% of the total fatty acid content, hence, the oil belongs to myristic acid category. Pig fat oil comprises 63.22% saturated acids (palmitic, lauric, myristic and stearic) and 36.75% unsaturated acids (oleic, linoleic and eicosatetraenoic). The dominant

monounsaturated fatty acid of the oil was Oleic acid, which accounted for 28.13% of the total fatty acid content, hence, the oil belongs to Oleic acid category. Nevertheless, the fatty acid components of the African pear and pig fat oil were found to be consistent with the fatty acids present in typical oils used for producing biodiesel as reported for cotton seed (Rashid *et al.*, 2009).

Table 3.2: Fatty acid composition of African pear (Ube) flesh oil and Pig fat oil

Fatty Acid	Carbon number	ppm weight for African pear oil	% weight for African pear oil	Ppm weight for pig fat (lard oil)	% weight for pig fat
Oleic acid	18 : 1	9.9733	17.60	18.8402	28.13
Lauric acid	12 : 0	9.9810	17.61	11.1193	16.60
Palmitic acid	16 : 0	7.2112	12.72	9.1141	13.61
Stearic acid	18 : 0	9.5877	16.92	9.6103	14.35
Myristic acid	14 : 0	14.1336	24.94	12.4960	18.66
Linoleic acid	18 : 2	4.3378	7.65	4.3389	6.480
Eiscosatetraenoic acid (ETA)	20 : 4	1.4328	2.52	1.4341	2.14

3.1.3 FTIR of the oils

The FTIR spectra of the pig fat (raw oil) and African pear oil was carried out in the range from 600 to 4000cm^{1} to study the functional groups in the raw pig fat and African pear flesh oil. The FTIR spectra results of the two raw oils as shown on table 3.3 and 3.4 indicates that both raw oils contain essential function group like Phenols, Alcohols, amines, amides, carboxylic acids, alkyl group and esters for both saturated and unsaturated compounds that made both oil good feedstock for biodiesel production.

Table 3.3: FTIR interpretation of the raw pig fat (Lard oil)

Peak value	Peak Intensity	Group and class	Bonds
3660.397	Strong	OH in alcohols and phenols	OH stretch
3328.65	Strong	-OH in alcohols and phenols	OH Stretch
3233.279	Medium-strong	≡CH in acetylenes	≡CH stretc
2971.036	Medium-strong	CH_3 and CH_2 in aliphatic compounds	CH antisym and sym stretching
2632.456	Weak-medium	CHO in aldehydes	Overtone of CH bending
2473.964	Very broad	-OH in carboxylic acids	H-bonded OH stretch
2065.337	Medium	$N=N^{+}=N^{-}$ in azides	$N=N^{+}=N^{-}$ antisym stretch
1857.131	Strong	C=O in β-lactones	C=O stretch
1632.373	Strong	C=O and NH_2 in primary amides	Two bands from C=O stretch and NH_2 deformation
1437.149	Medium	OH in carboxylic acids	OH bending
1226.468	Very strong	C-O stretch in acids, esters	C-O stretch
879.6799	Very strong	1,2,4- trisubt. Benzene	CH out of plane deformation (two bands)
753.1725	Strong	0-disubst. Benzene	CH out of plane deformation

Table 3.4: For FTIR interpretation of the raw African pear (Ube) oil

Peak value	Peak Intensity	Group and class	Bonds
3428.771 3279.955 3162.702	Medium-strong	-NH_2 in aromatic amines, primary amines and amides	NH stretch

© MAY 2026 | IRE Journals | Volume 9 Issue 11 | ISSN: 2456-8880
DOI: https://doi.org/10.64388/IREV9I11-1718212

3038.395	Medium	=CH in aromatic and unsaturated hydrocarbons	=CH-H Stretch
2913.474	Medium-strong	CH_3 and CH_2 in aliphatic compounds	CH antisym and sym stretching
2678.233	Weak-medium	CHO in aldehydes	Overtone of CH bending
2556.349	Medium	OH in phosphorus oxyacids	Associated OH stretching
2449.102	Very broad	OH in carboxylic acids	H-bonded OH stretch
2270.674	Medium-strong	C≡N in nitrils or C≡C alkynes	C≡N or C≡C stretch
2085.075	Medium	N=N+=N- in azides	N=N+=N- antisym stretch
1846.119	Strong	C=O in β-lactones	C=O stretch
1619.077	Strong	C=O and NH2 in primary amides	Two bands from C=O stretch and NH2 deformation
1385.009	Strong	NO2 in aromatic nitro compounds	NO2 antisym stretch
			NH3+ deformation
	Strong	NH3+ in amino acids or hydrochlorides	
			N=N-O antisym stretch
	Medium-strong		
		N=N-O in azoxy compounds	
1176.687	Strong	C-O in acids, esters	C-O stretch
826.2678	Very strong	1,3,5-trisubstituted benzene	CH out of plane deformation
699.7571	Strong	C-C-CHO in aldehydes	C-C-CHO bending

3.2 Characterization Result of the Catalyst

3.2.1 Scanning Electron Microscope

Figure 3.1a and 3.1b was scanning electron micrographs of the raw and calcined cow bone, which were magnified 500 times respectively. Comparison of the two micrographs shows that there was a significant difference between the morphologies of the raw and calcinated cow bone powder compositions. Interconnected granular microporosity was observed in the cow bone calcinated at 900ºC, favouring its effectiveness as a catalyst

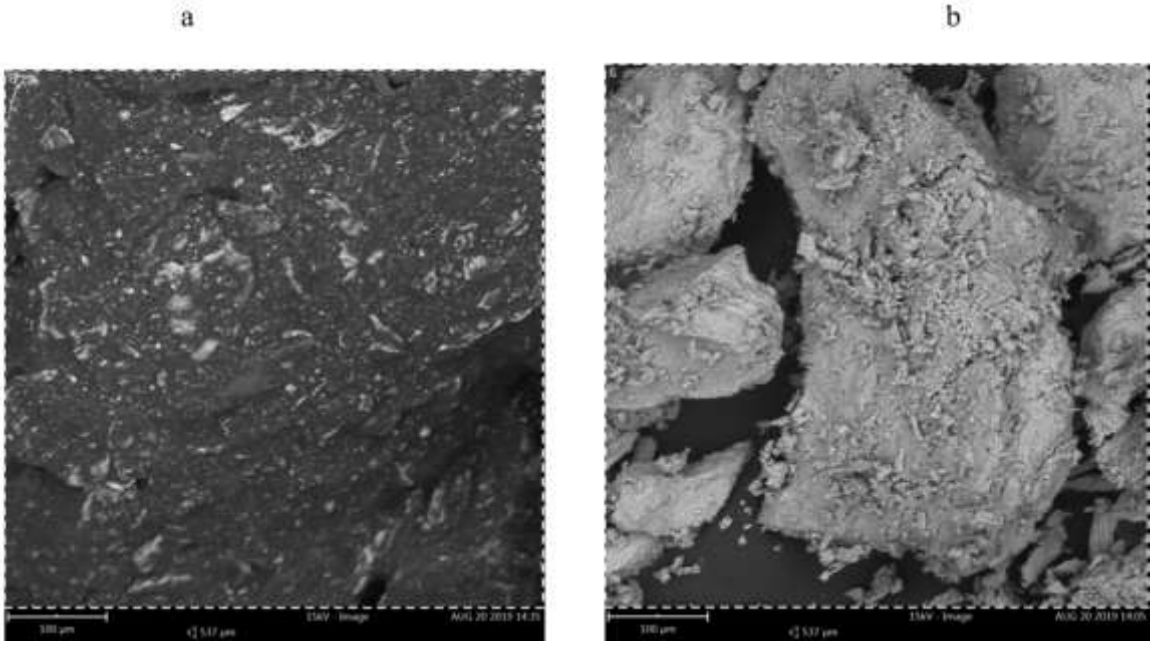

Figure 3.1: Scanning Electron Microscope (SEM) of (a) raw bone (b) calcinated cow bone

3.2.2 Thermogrametric analysis of the bone

Figures 3.2a and 3.2b shows TG curve of the catalyst, which declined slowly when temperature rose from 0

© MAY 2026 | IRE Journals | Volume 9 Issue 11 | ISSN: 2456-8880
DOI: https://doi.org/10.64388/IREV9I11-1718212

to 200 ° C. It explained that the residual moisture of catalyst flowed away gently. As the temperature increases from 200 to 450 °C, the TG curve dropped sharply, which made collagen gradually reduced. When the temperature continuously rose from 450 to 900 °C, the TG curve declined gradually trending to a smooth and steady phase. This indicated that thermal decomposition temperature of the catalyst was higher, so its stability was better.

TG characterization exposited that pyrolysis temperature of the cow bone was higher, so it had better stability. Cow bone catalyst could be reused and its structure still retained its original form after recycling.

Figure 3.2a: Showing the TGA result analysis for raw cow bone

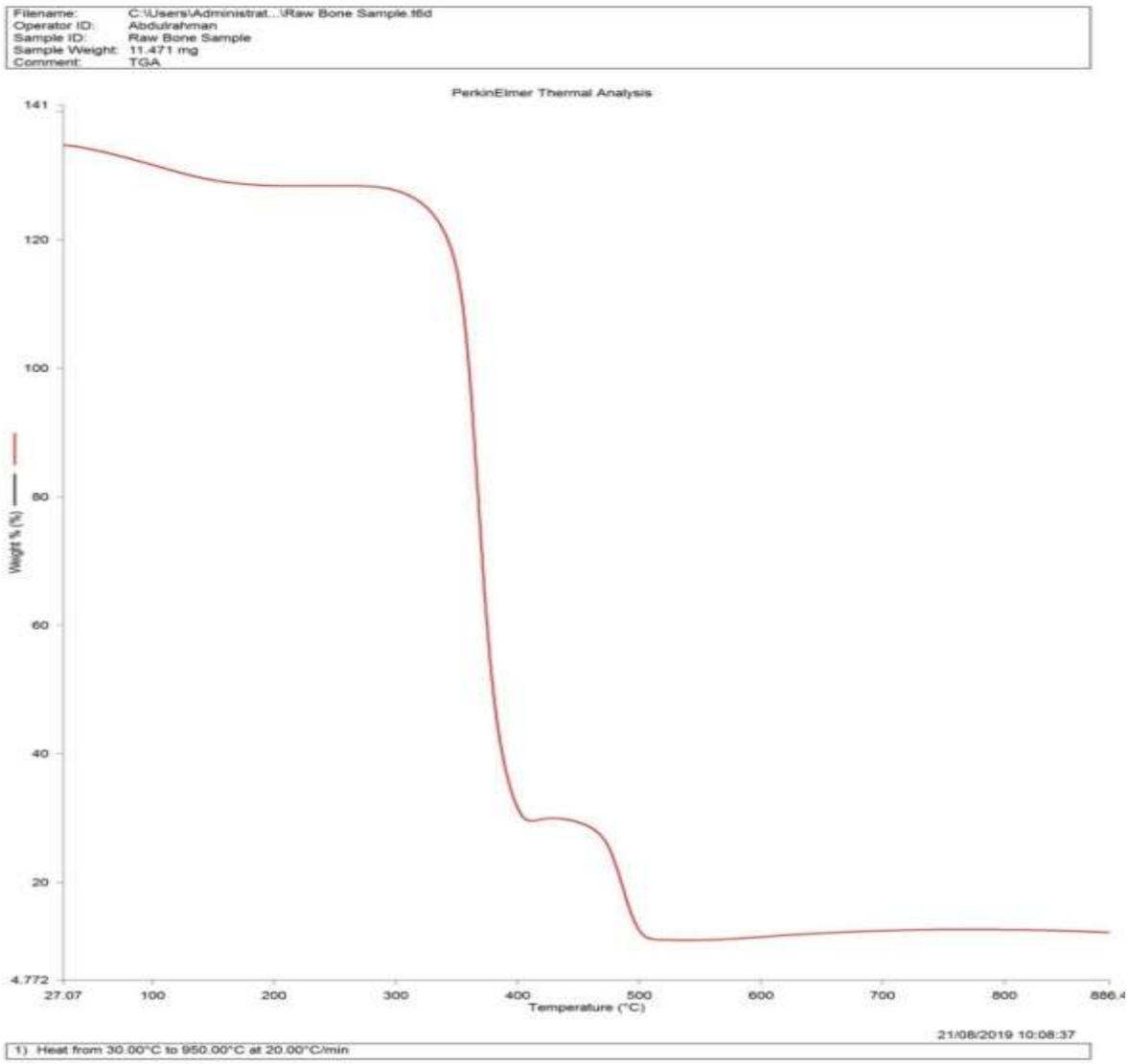

© MAY 2026 | IRE Journals | Volume 9 Issue 11 | ISSN: 2456-8880
DOI: https://doi.org/10.64388/IREV9I11-1718212

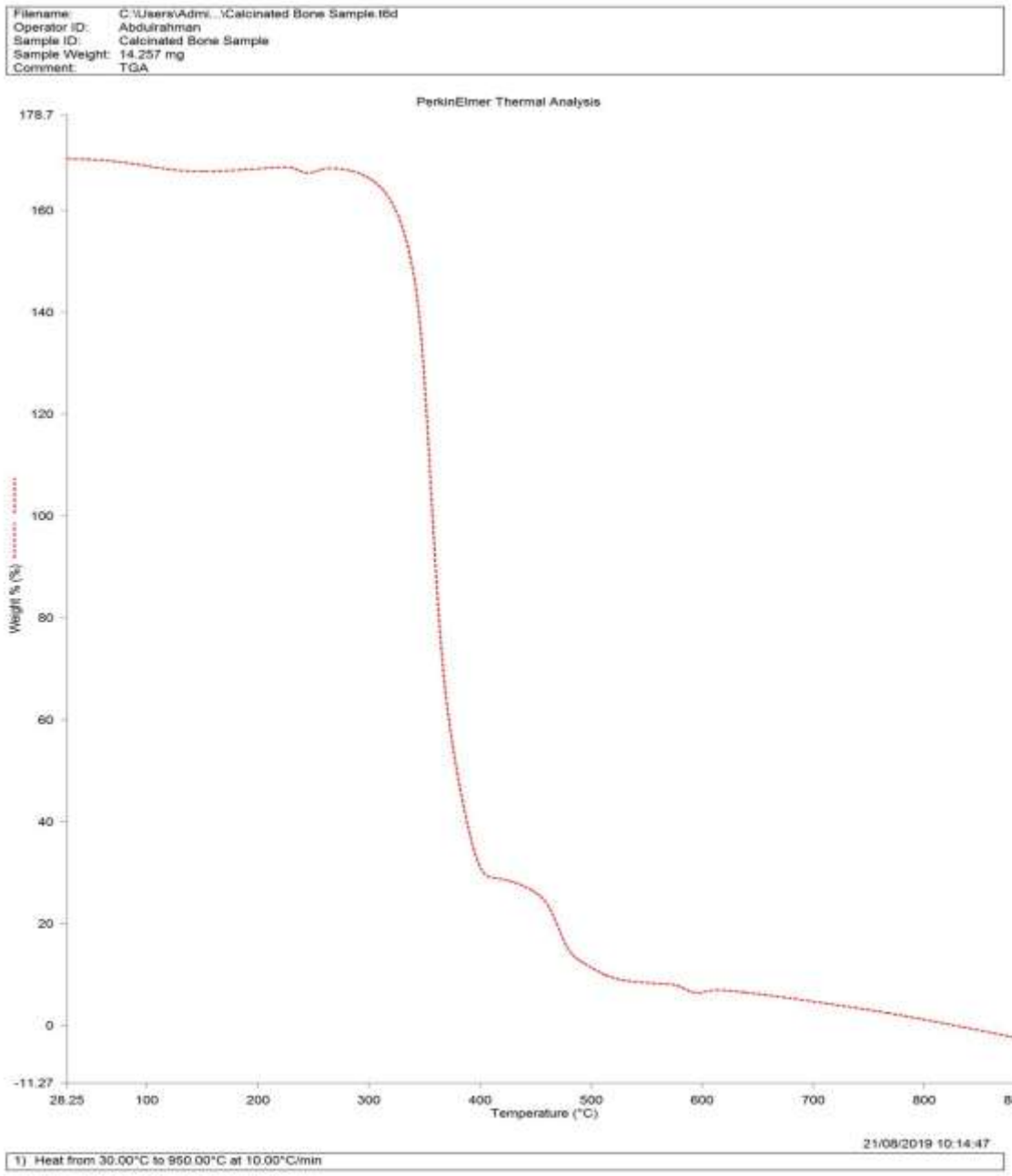

Figure 3.2b: Showing the TGA result analysis for calcinated cow bone

3.2.3 X-ray diffraction of the catalyst

Figure 3.3 shows X-ray diffraction diagrams of raw and calcined samples of cow bone. It could be seen that the characteristic diffraction peak of the calcined cow bone was almost completely the same with the raw sample. There was no other impurity peak, which meant that purity of the calcined bone was high. The peaks were sharp. These explained the crystallinity of the calcinated bone sample better in this experiment, having the macroscopic composition and microscopic structure of natural bone. That implied that the process of calcination of bones could be used for preparation of catalyst.

© MAY 2026 | IRE Journals | Volume 9 Issue 11 | ISSN: 2456-8880
DOI: https://doi.org/10.64388/IREV9I11-1718212

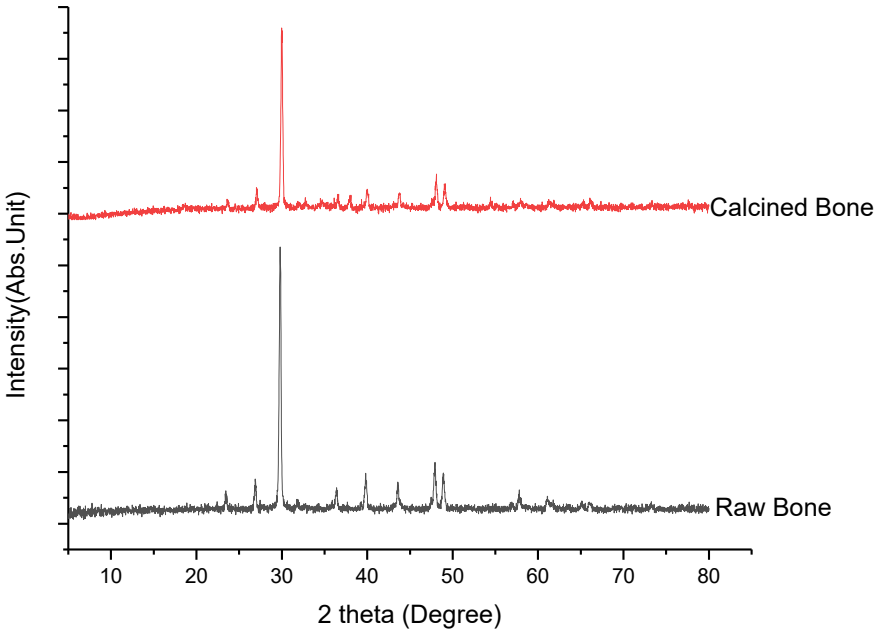

Figure 3.3: Showing the X-Ray diffraction of the raw and calcinated cow bone.

3.2.4 Fourier transform infra-red Analysis of the catalyst

Table 3.5 and 3.6 shows the functional groups that were detected in the raw and calcined cow bone using IR at wavelength range of 600nm to 4000nm. There was a wide absorption peak between3600 and 3200 cm^{-1}, which was caused by -OH stretching vibration peak of hydrogen-bond association and absorption peak of adsorption of water on the surface of the raw cow bone. The weak absorption peak at 1619 or 1667cm^{-1} explained that the surface of bone adsorbed water molecules. The raw structure of the raw sample and calcined cow bone were basically the same. The only difference between was absorption peak disappearing at 2921 cm^{-1}. The absorption peak at 2977.484 cm^{-1} was also-OH stretching vibration peak of hydrogen-bond association, which indicated that hydrogen bond structure of the calcined bone was not damaged in calcinations process.

IR characterization indicated that the calcinated cow bone had the macroscopic composition and microstructure of natural bone. That is, the product cow bone catalyst has application value, which the process of calcinations of animal bone can prepare. In the spectra of the raw and calcined samples, absorption maxima at 712, 875,1430, and 1470 cm^{-1}, characteristic for vibrations of C-O bonds in the composition of calcium carbonate (CC), are also recorded.

Table 3.5: The functional group for the raw cow bone

Peak value	Peak Intensity	Group and class	Bonds
3653.909	Strong	OH in alcohols and phenols	OH stretch
3283.8	Medium-strong	≡CH in acetylenes	≡CH stretch
3045.742	Medium	CH_3 attached to O or N	CH antisym and sym stretching
2605.518	Weak-medium	CHO in aldehydes	Overtone of CH bending
2492.348	Very broad	-OH in carboxylic acids	H-bonded OH stretch
2126.623	Medium	C≡N in thiocyanate	C≡N in antisym stretch
1833.982	Strong	C=O in β-lactones	C=O stretch
1122.735	Very strong	C-O stretch in acids, esters	C-O stretch

© MAY 2026 | IRE Journals | Volume 9 Issue 11 | ISSN: 2456-8880
DOI: https://doi.org/10.64388/IREV9I11-1718212

Table 3.6: The FTIR functional groups in the calcined cow bone

Peak value	Peak Intensity	Group and class	Bonds
3212.706	Medium-strong	≡CH in acetylenes	≡CH stretch
2977.484	Medium-Strong	CH_3 and CH_2 in aliphatic	CH antisym and sym stretching
2637.676	Weak-medium	CHO in aldehydes	Overtone of CH bending
2458.518	Very broad	-OH in carboxylic acids	H-bonded OH stretch
2130.463	Medium	C≡N in thiocyanate	C≡N in antisym stretch
1833.982	Strong	C=O and NH_2 in primary amides	C=O stretch

3.2.5 X-ray fluorescence (XRF) analysis of the catalyst

Table 3.7 and 3.8 below is for the elemental composition of the raw and calcinated cow bone, which indicates that both contained enough elements that are important components for catalytic and other activities. From the result below calcinated bone appeared to contain more of the following elements at a higher concentration (Ca, P, Mg) compared to the raw sample. This indicates the composition that enables the bone to act as catalyst.

Table 3.7: The elemental composition of the raw cow bone

Element Symbol	Atomic Conc.	Weight Conc.
C	95.68	85.81
Ca	2.11	6.33
Zr	0.67	4.57
P	0.74	1.71
Na	0.23	0.39
Mg	0.20	0.37
Si	0.12	0.25
Al	0.11	0.23
K	0.06	0.18
S	0.07	0.17

Table 3.8: The elemental composition of the calcinated cow bone

Element Symbol	Atomic Conc.	Weight Conc.
Zn	0.45	0.68
Ca	57.03	53.09
Zr	11.93	25.28
P	19.28	13.87
Na	4.06	2.17
Mg	2.82	1.59
Si	0.79	0.51
Al	1.57	0.98
K	0.60	0.55
S	1.11	0.83
Fe	0.18	0.23
V	0.19	0.22
Ti	0.00	0.00

3.2.6 BET analysis of the catalyst

According to the measured values of BET in Table 3.9 below specify surface area, pore volume, and pore diameter of the cow bones were similar. Based on classification of pore diameter: micropore (<2 nm), mesoporous (2~50 nm), macropore (> 50 nm) (ref), the cow bone pertained to mesoporous due to the pore diameter value2.8 nm. It showed that the product had

a significant surface area. The larger the surface area is, the stronger the surface effect, such as surface activity, surface adsorption capacity, catalytic ability, and so on. So, this product could be used for different catalytic process.

Table 3.9: The BET analysis for specific surface area of the raw and calcined cow bone

Sample	Surface area (m^2/g)	Pore Volume(cc/g)	Pore diameter(nm)
Raw cow bone	147.511	0.134	2.800
Calcined cow bone	168.674	0.146	2.640

3.3
Optimization of Transesterification of Lard Oil by RSM

A five-level four-factor central composite design CCD requiring 30 experiments was employed for the optimization of the transesterification process. The result of the process parameters such as effect of temperature, reaction time, amount of catalyst, methanol/oil on the yield of biodiesel from pig fat (Lard oil) was conducted using the design matrix as shown in Table 3.2. The results showed their effect on the transesterification process and, the ANOVA for responses conducted as shown in Table 3.10 below. The FAME content obtained was in the range from 52.73% to 96.426%. Atoptimal temperature (50ºC), time(135mins) and methanol ratio (10:1) the optimization of FAME yield was further verified in the laboratory using the Predicted optimal yield generated from the optimization of the FAME yield from range (52.73% to 96.426%) and the conditions as shown on Table 3.12.

Table 3.10 shows the regression analysis of the RSM in which the three linear terms (*A* and D), and the four quadratic terms (A^2, B^2, C^2, D^2) were all significant model terms at 95%confidence level as the significance determined by *p* value i.e., ($p<0.05$). The second-order effects of A^2, C^2 and D^2 were most significant, all having *p*-value<0.0001. The Analysis of variance (ANOVA) as shown in Table 3.10 shows the model F value 18.36 with low probability value (*p*-value<0.0001) implies a high significance for the regression model. The coefficient of determination (R^2) measures the goodness of the fit of the model, greater than 0.80 was desirable (Betiku *et al*., 2013). The R^2 value of 0.9449 which means that model could explain (94.49) of the variation in FAME content, which is attributed to the independent variables, and only 5.5%of the total variation is not explained by the model. It indicates the fitness of the model. The predicted $R^2$of 0.7130 was in reasonable agreement with the adjusted $R^2$of 0.8934 indicating that the regression model could be used to analyze trends of responses. The adjusted R^2 value is particularly useful when comparing models with a different number of terms. This comparison was, however, done in the background when model reduction was taking place (Noordin *et al*, 2004). Apart from that, the lack of fit *F*-value of 33.84 implies that lack of fit was not significant relative to pure error. Hence, there is only a merechance that a lack of fit F-value this large could occur due to noise factor such as human errors or experimental errors (Tan *et al*., 2010). The non-significant lack of fit shows the model is significant and indicates that the model equation is adequate for predicting FAME content under any sets of combination of the variables (Garai *et al*., 2013). The low coefficient of variation (6.56%) shows the reliability of experiments conducted (Yuan *et al*., 2008). Adequate precision measures the signal to noise ratio. Adequate precision of (12.4560) indicates an adequate signal as a ratio greater than 4 was desirable to navigate the design space excellently (Noordin *et al*., 2004). Multiple regression analysis of the experimental data gave the following second-order polynomial equation in terms of coded variables:

$$Y = 94.4081 + 2.34856 * A + 3.35342 * D + -10.3596 * A^2 + -4.63563 * B^2 + -9.67362 * C^2 + -8.26663 * D^2 \quad (3.1)$$

Where, *Y* represents percentage FAME content. Positive sign in front of the terms indicates the synergistic effect in increased FAME content, whereas a negative sign indicates the antagonistic effect (Santos *et al*., 2013). Model Eq. 4.1with linear term *A*, and *D* had a positive effect on FAME content whereas all quadratic terms A^2, B^2, C^2, D^2 had a negative effect on FAME content. The Variance Inflation Factor (VIF) did not exceed 1.05 for any of the terms in the quadratic equation. This reflects that there is no problem of multi co linearity (since VIF<10). In addition, the leverage for each response 0.583 was less than twice the average leverage and hence is acceptable (Narang *et al*., 2001).

© MAY 2026 | IRE Journals | Volume 9 Issue 11 | ISSN: 2456-8880
DOI: https://doi.org/10.64388/IREV9I11-1718212

Table 3.10: Analysis of Variance for Response surface analysis on Lard oil biodiesel

Source	Sum of Squares	DF	Mean Square	F- Value	Prob > F
Model	5799.90	14	414.28	18.36	< 0.0001
A	110.31	1	110.31	4.89	0.0430
B	3.04	1	3.04	0.1347	0.7187
C	25.82	1	25.82	1.14	0.3016
D	224.91	1	224.91	9.97	0.0065
AB	24.19	1	24.19	1.07	0.3169
AC	59.55	1	59.55	2.64	0.1251
AD	100.67	1	100.67	4.46	0.0518
BC	12.60	1	12.60	0.5587	0.4663
BD	3.151	1	3.15	0.1395	0.7140
CD	17.18	1	17.18	0.7617	0.3966
A^2	1001.67	1	1001.67	44.40	0.0001
B^2	200.56	1	200.56	8.89	0.0093
C^2	873.40	1	873.40	38.71	0.0001
D^2	637.81	1	637.81	28.27	0.0001
Residual	338.40	15	22.56		
Lack of fit	338.40	10	33.84		
Pure error	0.0000	5	0.0000		
Core Total	6138.30	29			

Std Dev	Mean	C.V %	R^2	Adjusted R^2	Predicted	Adeq precision
4.75	72.45	6.56	0.9449	0.8934	0.7130	12.4560

3.4
Effect of Process parameter on Lard oil FAME

The model was then further processed to generate the response surface plots using trial Version 12 of design expert and analyzed to understand the interactions among the variables followed by optimization of each variable for maximization of FAME content. Deterministic models enable researchers to predict and describe the dynamics of a system over space and time. The 3D response surface plots are generally the graphical representations of the regression (Eq. 4.1) which are shown in Fig. 3.5 – 3.10. Statistical analysis of the experimental data identified methanol ratio (D) as the most important variable in the response analysis. Table 3.10 shows the temperature and methanol to oil molar ratio, have a significant effect on the FAME content.

A line of unit slope, i.e. line of perfect fit with points corresponding to zero error between the predicted values and actual values as shown in Fig. 3.4 indicating that the model represents a relatively good

© MAY 2026 | IRE Journals | Volume 9 Issue 11 | ISSN: 2456-8880
DOI: https://doi.org/10.64388/IREV9I11-1718212

description of the experimental data regarding the yield of FAME. It could be seen from the graph that all the points are very close to the line of perfect fit hence, there is adequate correlation between the predicted values and the experimental values of the independent variable which further elaborated the adequacy of the model.

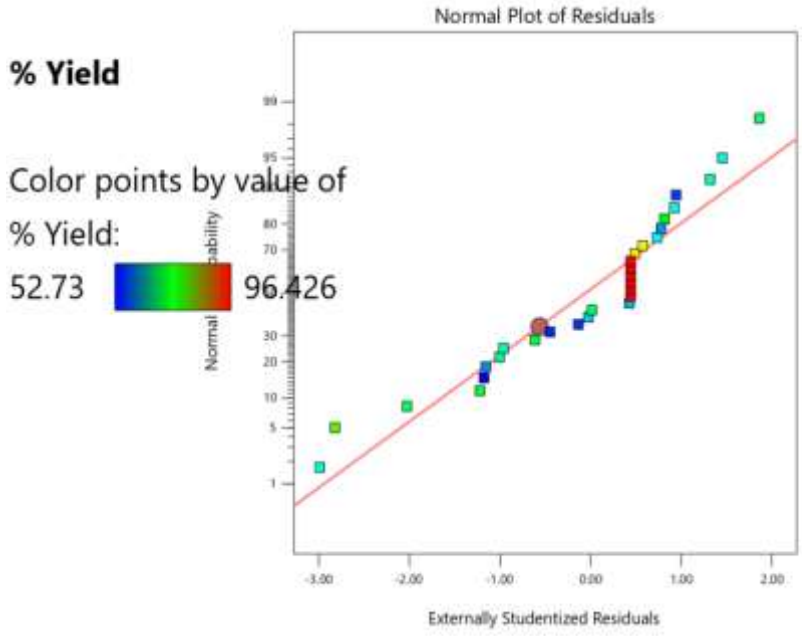

Figure 3.4: Straight line plot showing the predicted and actual experimental result for lard oil biodiesel

The effect of temperature and reaction time on FAME content at fixed value of molar ratio 10:1 and catalyst concentration 2.5%wt is shown in Fig. 3.5. It can be seen from Fig.3.5, at one axis, there is a linear increase in FAME content, while at the other axis, there is increase only up to an extent, which decreases thereafter. This indicates that a critical point for temperature is involved up to which reaction is favored and not so after that critical point. The percentage FAME content is lower at shorter times and increases as the time is increased to 135 min. Increasing the reaction time above 135 min showed no significant effect on the FAME content.

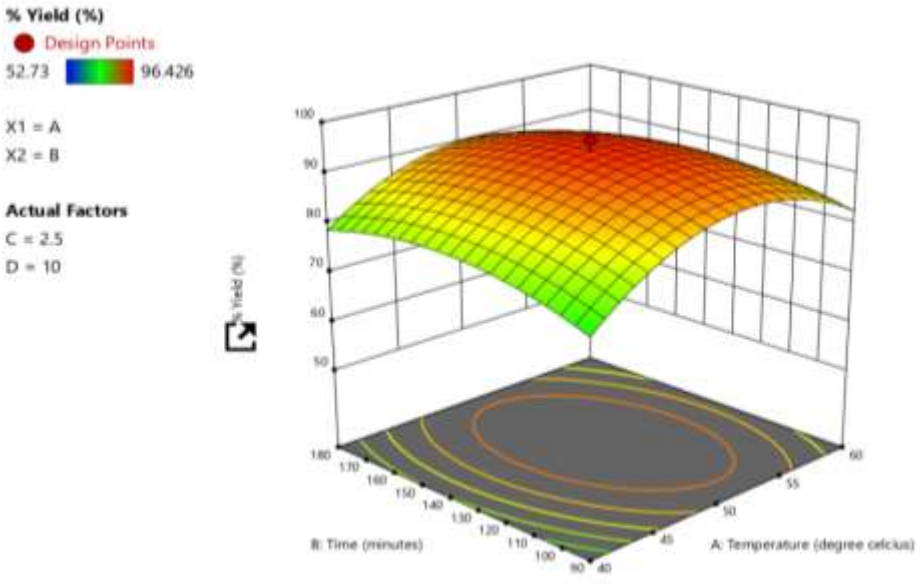

Figure 3.5: Surface plot of the interaction effect of temperature and time to FAME yield

© MAY 2026 | IRE Journals | Volume 9 Issue 11 | ISSN: 2456-8880
DOI: https://doi.org/10.64388/IREV9I11-1718212

The effect of temperature and catalyst concentration on FAME content at fixed value of molar ratio 10:1 and reaction time 135minsis shown in Fig. 3.6. It can be seen from Fig.3.6, at one axis, there is a linear increase in FAME content, while at the other axis, there is increase only up to an extent, which decreases thereafter. This indicates that a critical point for temperature is involved up to which reaction is favored and not so after that critical point and, from the experiment the critical temperature point of the reaction is 50^0C. The percentage FAME content is lower at lower catalyst concentration and increases as the catalyst concentration is increased to 2.5%wt. Increasing the catalyst concentration above 2.5%wt showed no significant increase effect on the FAME content and, further addition of catalyst found negative effect on FAME content. This may be due to fact that addition of an excess amount of catalyst, give rise to the formation of an emulsion, which has increased the viscosity and led to the formation of gel. Chin *et al.,* 2009, found that higher catalyst concentration may make the reactant mixture more viscous, which would increase the mass transfer resistance to the reaction system.

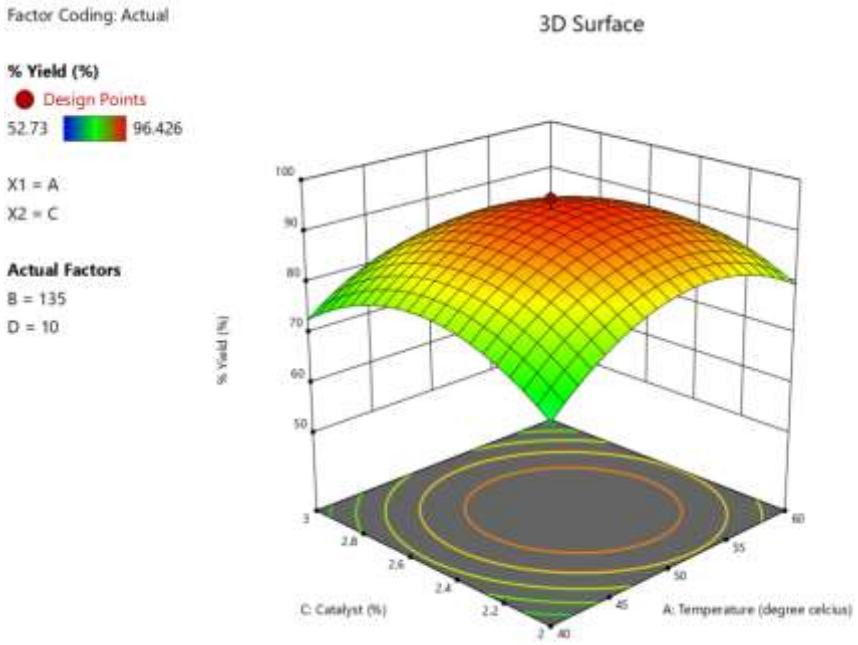

Figure 3.6: Surface plot of the interaction effect of temperature and catalyst to FAME yield

The simultaneous dependence of FAME content on the molar ratio and temperature is shown in Fig. 3.7. While, the other two process parameters are maintained at their zero levels. At lower value of molar ratio, FAME content is less even at higher temperature. As the molar ratio increased, FAME content also increased with increase in temperature. However, the maximum FAME content is obtained at molar ratio of 10:1 and temperature of 50^0C. Higher quantities beyond 10:1of methanol to oil molar ratio exhibits negative effect on FAME content, as it was clear by decreasing response with the increase in the molar ratio above 10:1. This is because, at molar ratios of methanol/oil higher than 10:1, separation of esters from glycerol was problematic. A molar ratio of 6:1 is generally considered the most appropriate for methanol. Although, in this work, we found molar ratio 10:1 to be best for methanolysis of Lard oil. This is because, of the predominance of the esterification reaction at the initial phase, to transesterify the remaining FFA acids present in the oil sample which can consume the methanol present in the reaction mixture at the initial stage of reaction and hence the amount of methanol available for the transesterification may not be sufficient to drive the reaction forward for the longer time. The second possible reason may be the evaporation of methanol during the reaction stage, which was condensed back to the reaction mixture. Hence, every time the same amount of methanol was not available for the reaction to happen in forward direction. Nevertheless, the results are quantitatively similar to those of literature where author (Azjargal *et al.,* 2012) reported 10:1 methanol/oil molar ratio for rubber seed oil biodiesel production.

© MAY 2026 | IRE Journals | Volume 9 Issue 11 | ISSN: 2456-8880
DOI: https://doi.org/10.64388/IREV9I11-1718212

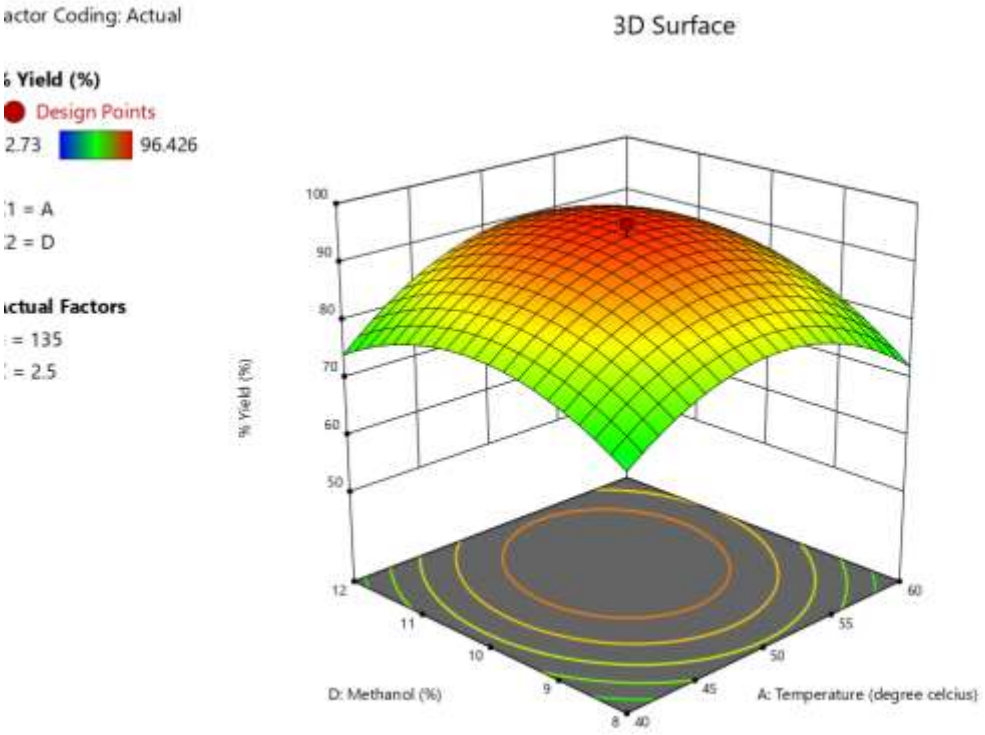

Figure 3.7: The surface plot of the interaction effect of temperature and methanol to FAME yield.

The effect of different reaction time and catalyst concentration on FAME content at fixed value of molar ratio 10:1 and temperature 50^{O}Cis shown in Fig. 3.8. It can be seen from Fig. 3.8, at one axis, there is a linear increase in FAME content, while at the other axis, there is increase only up to an extent, which decreases thereafter. This indicates that a critical point for time of reaction is involved up to which reaction is favored and not so after that critical point. The percentage FAME content is lower at shorter times and increases as the time is increased to 135 min. Increasing the reaction time above 135 min showed no significant effect on the FAME content. Our results are not in agreement with Anand et al. (2016), who investigated an optimum reaction time of 90mins at 60ºC for production of biodiesel by transesterification of Lard oil. The variations in our analysis might be due to the different catalyst type and concentration.

.

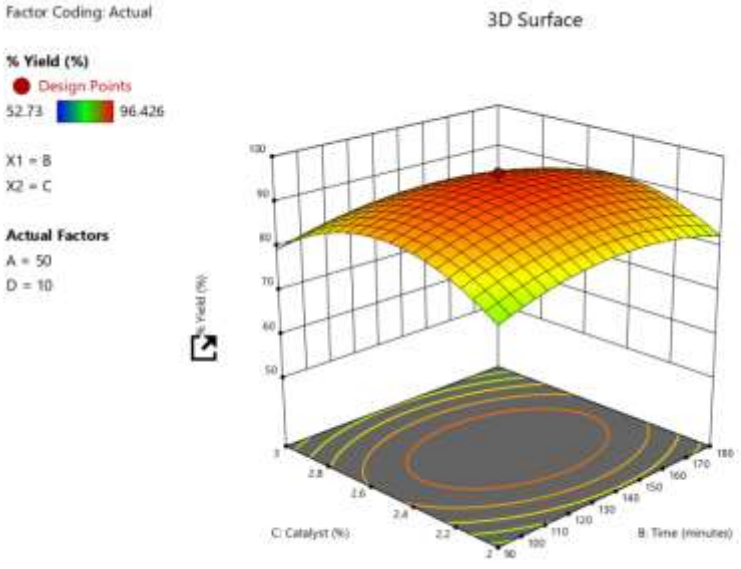

Figure 3.8: Showing surface plot of interaction effect of time and catalyst concentration to FAME yield.

© MAY 2026 | IRE Journals | Volume 9 Issue 11 | ISSN: 2456-8880
DOI: https://doi.org/10.64388/IREV9I11-1718212

The simultaneous dependence of FAME content on the time of reaction and molar ratio is shown in Fig.3.9. At lower value of molar ratio, FAME content is less even at higher time of reaction. As the molar ratio increased to 10:1, FAME content also increased with increase in time of reaction. However, the maximum FAME content is obtained at molar ratio of 10:1 and reaction time of 135mins.

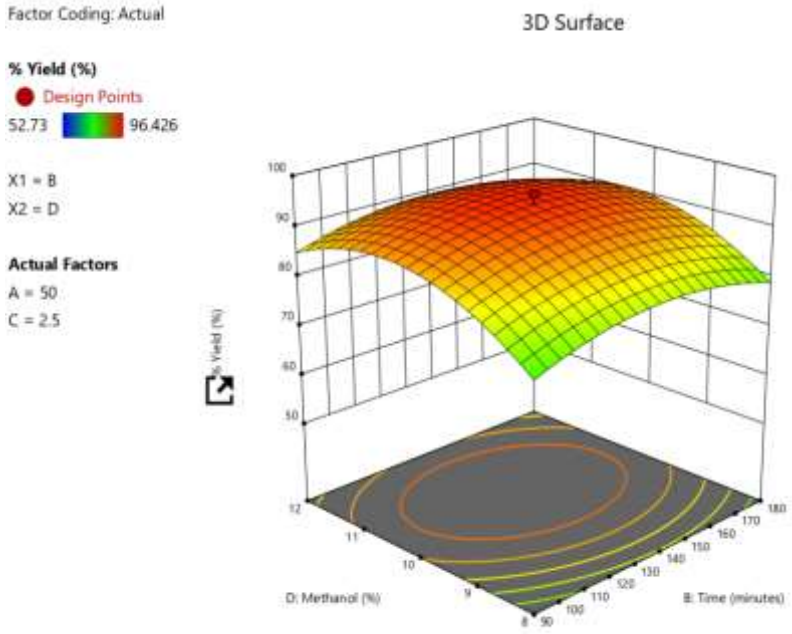

Figure 3.9: Showing surface plot of the interactive effect of time and methanol to FAME yield.

The simultaneous dependence of FAME content on the molar ratio and catalyst concentration is shown in Fig.3.10 While, the other two process parameters are maintained at their zero levels. At lower value of molar ratio, FAME content is less even at higher catalyst concentration. As the molar ratio increased from to 10:1, FAME content also increased with increase in catalyst concentration. However, the maximum FAME content is obtained at molar ratio of 10:1 and catalyst concentration of 2.5%wt. Higher quantities beyond 10:1of methanol to oil molar ratio exhibits negative effect on FAME content, as it was clear by decreasing response with the increase in the molar ratio. This is because, at molar ratios of methanol/oil higher than 10:1, separation of esters from glycerol was problematic.

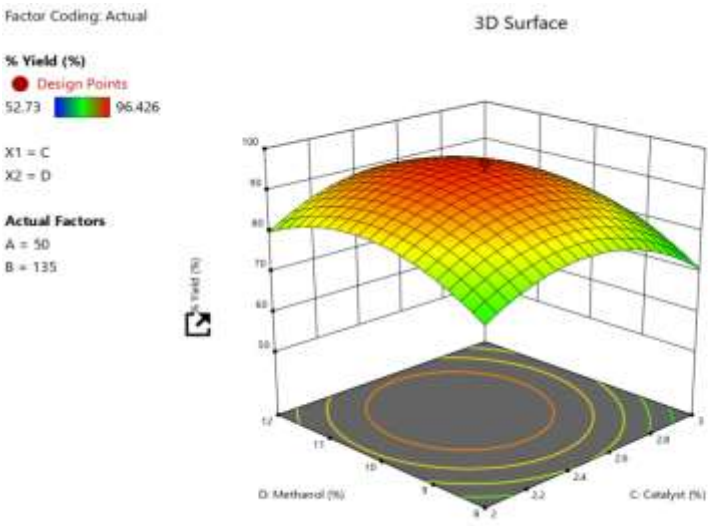

Figure 3.10: Showing surface plot of interaction effect of catalyst methanol to FAME yield.

3.5
Optimization of the Transesterification Process on African Pear Oil Biodiesel

A five-level four-factor central composite design CCD requiring 30 experiments was employed for the optimization of the transesterification process. The result of the process parameters such as effect of temperature, reaction time, amount of catalyst, methanol/oil on the yield of biodiesel from African pear (Ube) oil were conducted using the design matrix as shown in table 2.3. The results showed the effect of the process parameters on the transesterification process and, the ANOVA for responses conducted as shown in table 3.11 below. The FAME content obtained was in the range from 50.42 to 92.35. At optimal temperature (50^0C), time(135mins) and methanol ratio (10:1) the optimization of FAME yield was further verified in the laboratory using the Predicted optimal yield generated from the optimization of the FAME yield from range (50.42% to 92.35%) and conditions as shown on table 3.13.

Table 3.11 shows the regression analysis of the RSM in which the one linear term (D), and the four quadratic terms (A^2, B^2, C2, D^2) were all significant model terms at 95%confidence level as the significance determined by p value i.e., (p <0.05). The second-order effects of $A^2$and C^2 were most significant, both having p-value <0.0001. The Analysis of variance (ANOVA) as shown in Table 3.11 shows the model F value 15.22 with low probability value (p-value<0.0001) implies a high significance for the regression model. The coefficient of determination (R^2) measures the goodness of the fit of the model, greater than 0.80 was desirable (Betiku *et al*., 2013). The R^2 value of 0.9342 which means that model could explain (93.42) of the variation in FAME content, which is attributed to the independent variables, and only 6.56%of the total variation is not explained by the model. It indicates the fitness of the model. The predicted R^2 of 0.6946 was in reasonable agreement with the adjusted R^2 of 0.8728 indicating that the regression model could be used to analyze trends of responses. The adjusted R^2 value is particularly useful when comparing models with a different number of terms. This comparison was, however, done in the background when model reduction was taking place (Noordin *et al*, 2004). Apart from that, the lack of fit F-value of 38.07 implies that lack of fit was not significant relative to pure error. Hence, there is only a merechance that a lack of fit F-value this large could occur due to noise factor such as human errors or experimental errors (Tan et al., 2010). The non-significant lack of fit shows the model is significant and indicates that the model equation is adequate for predicting FAME content under any sets of combination of the variables (Garai *et al.*, 2013). The low coefficient of variation (7.41%) shows the reliability of experiments conducted (Yuan *et al.*, 2008). Adequate precision measures the signal to noise ratio. Adequate precision of (10.9718) indicates an adequate signal as a ratio greater than 4 was desirable to navigate the design space excellently (Noordin *et al*., 2004). Multiple regression analysis of the experimental data gave the following second-order polynomial equation in terms of coded variables:

$$Y = 89.381 + 3.14861 * D + -10.1087 * A^2 + -5.54375 * B^2 + -9.31375 * C^2 + -7.12625 * D^2 \text{ -------} \quad (3.2)$$

Table 3.11: Analysis of Variance for Response surface analysis on African pear oil biodiesel

Source	Sum of Squares	DF	Mean Square	F- Value	Prob > F
Model	5408.54	14	386.32	15.22	< 0.0001
A	102.62	1	102.62	4.04	0.0627
B	0.8370	1	0.8370	0.0330	0.8583
C	22.871	1	22.87	0.9012	0.3575
	198.27	1	198.27	7.81	0.0136
AB	3.07	1	3.07	0.1210	0.7328
AC	75.91	1	75.91	2.99	0.1043
AD	79.88	1	79.88	3.15	0.0964
BC	5.16	1	5.16	0.2035	0.6584
BD	9.32	1	9.32	0.3671	0.5537
CD	0.5293	1	0.5293	0.0209	0.8871
A^2	953.74	1	953.74	37.57	< 0.0001

© MAY 2026 | IRE Journals | Volume 9 Issue 11 | ISSN: 2456-8880
DOI: https://doi.org/10.64388/IREV9I11-1718212

B^2	286.84	1	286.84	11.30	0.0043
C^2	809.63	1	809.63	31.90	< 0.0001
D^2	473.98	1	473.98	18.67	0.0006
Residual	380.75	15	25.38		
Lack of fit	380.75	10	38.07		
Pure error	0.0000	5	0.0000		
Core Total	5789.29	29			

Std Dev	Mean	C.V %	R^2	Adjusted R^2	Predicted	Adeq precision
5.04	67.99	7.41	0.9342	0.8728	0.6946	10.9718

3.6
Effect of Process Parameter on African Pear Oil FAME

The model was then further processed to generate the response surface plots using trial Version 12 of design expert and analyzed to understand the interactions among the variables followed by optimization of each variable for maximization of FAME content. Deterministic models enable researchers to predict and describe the dynamics of a system over space and time. The 3D response surface plots are generally the graphical representations of the regression (Eq. 3.2) which are shown in Fig. 3.12 – 3.17. Statistical analysis of the experimental data identified methanol ratio (D) as the most important variable in the response analysis (*Ibiam et al.*, 2025). Table 3.11shows the methanol to oil molar ratio, have a significant effect on the FAME content.

A line of unit slope, i.e. line of perfect fit with points corresponding to zero error between the predicted values and actual values as shown in Fig. 3.11 indicating that the model represents a relatively good description of the experimental data regarding the yield of FAME. It could be seen from the graph that all the points are very close to the line of perfect fit hence, there is adequate correlation between the predicted values and the experimental values of the independent variable which further elaborated the adequacy of the model.

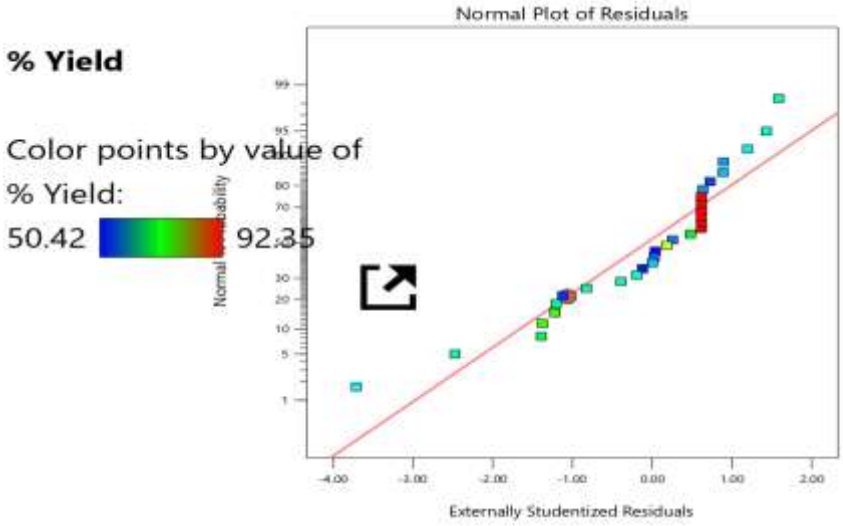

Figure 3.11: Straight line plot showing the predicted and actual experimental for African pear oil biodiesel

The simultaneous effect of temperature and reaction time on FAME content at fixed value of molar ratio 10:1 and catalyst concentration 2.5%wt is shown in Fig. 3.12. It can be seen from Fig.3.12, at one axis, there is a linear increase in FAME content, while at the other axis, there is increase only up to an extent, which decreases thereafter. This indicates that a critical point for temperature is involved up to which reaction is favored and not so after that critical point. The percentage FAME content is lower at shorter times and increases as the time is increased to 135 min. Increasing the reaction time above 135 min showed no significant effect on the FAME content.

© MAY 2026 | IRE Journals | Volume 9 Issue 11 | ISSN: 2456-8880
DOI: https://doi.org/10.64388/IREV9I11-1718212

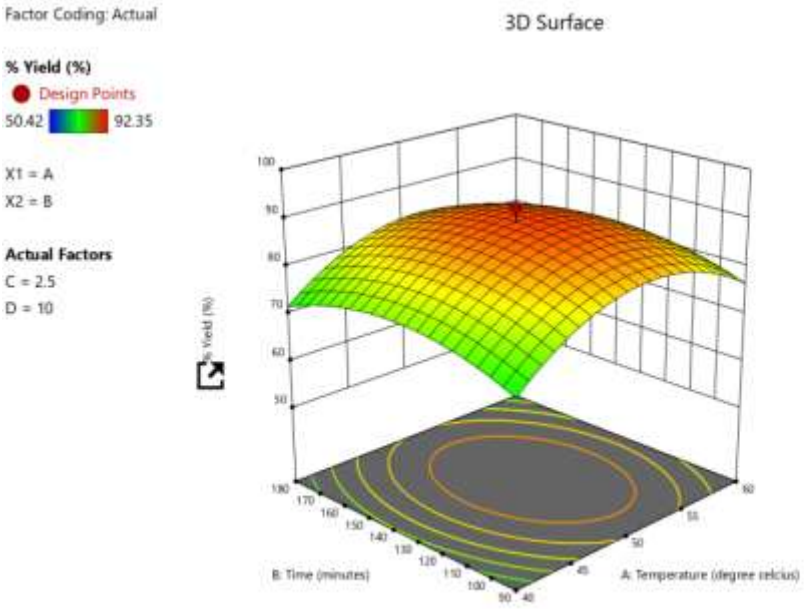

Figure 3.12: Showing surface plot of interaction effect of temperature and time of FAME yield on African pear oil.

It can be seen from Fig.3.13, at one axis, there is a linear increase in FAME content, while at the other axis, there is increase only up to an extent, which decreases thereafter. This indicates that a critical point for temperature is involved up to which reaction is favored and not so after that critical point and, from the experiment the critical temperature point of the reaction is 50^0C. The percentage FAME content is lower at lower catalyst concentration and increases as the catalyst concentration is increased to 2.5%wt. Further addition of catalyst beyond 2.5%wt found negative effect on FAME content. This may be due to fact that addition of an excess amount of catalyst, give rise to the formation of an emulsion, which has increased the viscosity and led to the formation of gel. Chin *et al.,* 2009, found that higher catalyst concentration may make the reactant mixture more viscous, which would increase the mass transfer resistance to the reaction system.

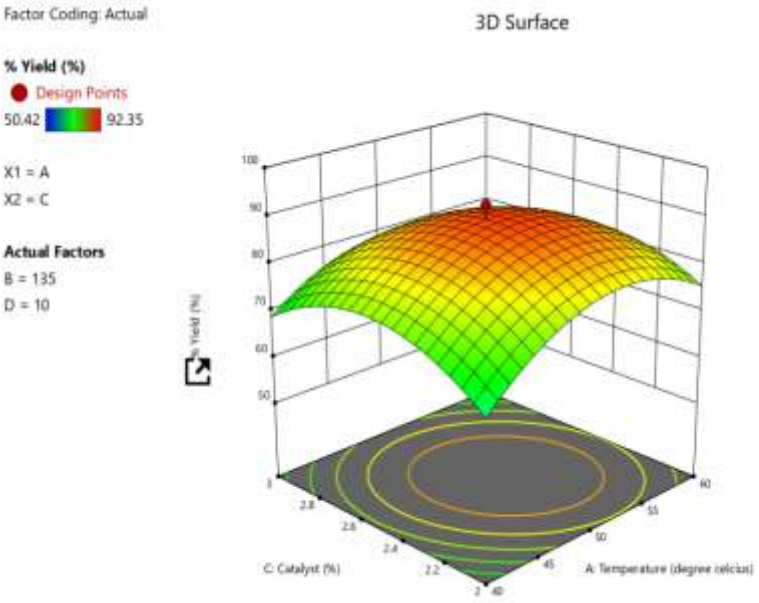

Figure 3.13: Showing surface interaction plot of temperature and catalyst concentration to FAME yield on African pear oil biodiesel.

© MAY 2026 | IRE Journals | Volume 9 Issue 11 | ISSN: 2456-8880
DOI: https://doi.org/10.64388/IREV9I11-1718212

The dependence of FAME content on the molar ratio and temperature is shown in Fig. 3.14. While, the other two process parameters are maintained at their zero levels. At lower value of molar ratio, FAME content is less even at higher temperature. As the molar ratio increased, FAME content also increased with increase in temperature. However, the maximum FAME content is obtained at molar ratio of 10:1 and temperature of 50ºC. Higher quantities beyond 10:1of methanol to oil molar ratio exhibits negative effect on FAME content, as it was clear by decreasing response with the increase in the molar ratio above 10:1. This is because, at molar ratios of methanol/oil higher than 10:1, separation of esters from glycerol was problematic. The results are quantitatively different to those of literature where author (Ofoefule *et al.,*201) reported 6.86:1 methanol/oil molar ratio for African pear oil biodiesel production.

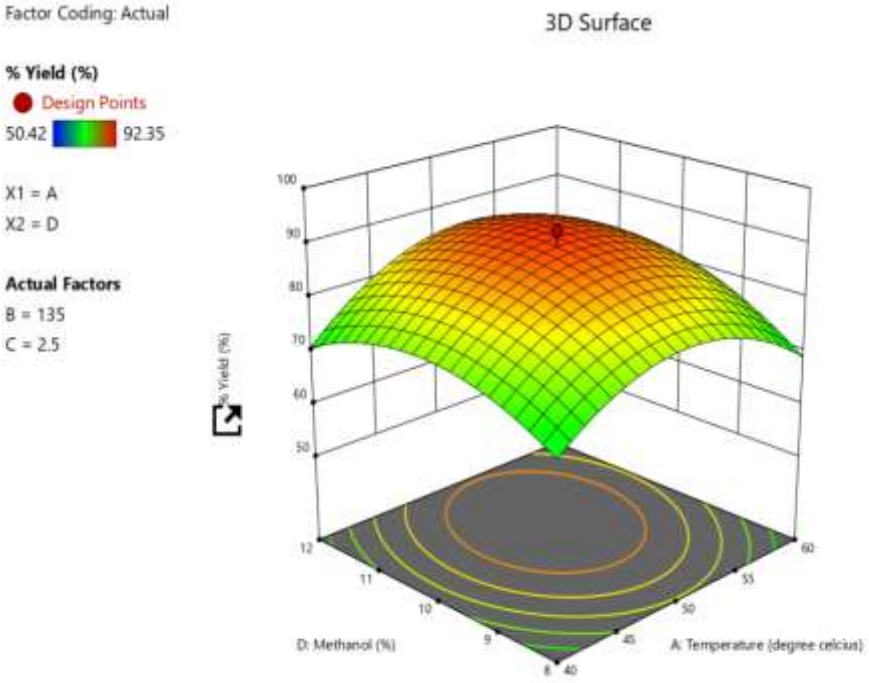

Figure 3.14: Surface interaction plot of temperature and methanol – oil ratio to FAME yield on African pear oil biodiesel.

The effect of different reaction time and catalyst concentration on FAME content at fixed value of molar ratio 10:1 and temperature 50ºCis shown in Fig. 3.15. It can be seen from Fig. 3.15, at one axis, there is a linear increase in FAME content, while at the other axis, there is increase only up to an extent, which decreases thereafter. This indicates that a critical point for time of reaction is involved up to which reaction is favored and not so after that critical point. The percentage FAME content is lower at shorter times and increases as the time is increased to 135 min. Increasing the reaction time above 135 min showed no significant effect on the FAME content (*Ibiam et al.*, 2025).

© MAY 2026 | IRE Journals | Volume 9 Issue 11 | ISSN: 2456-8880
DOI: https://doi.org/10.64388/IREV9I11-1718212

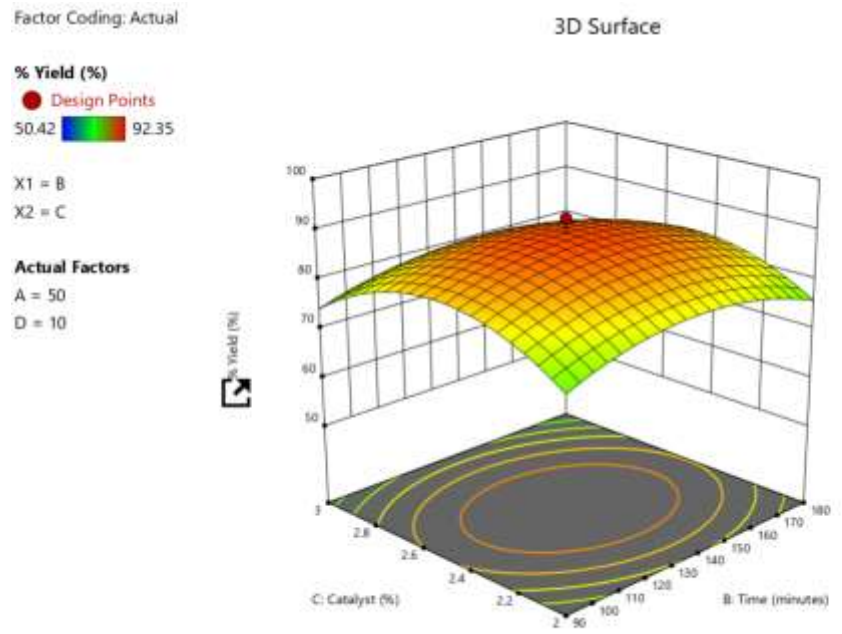

Figure 3.15: Surface interaction plot of time of reaction and catalyst concentration of FAME yield on African pear oil biodiesel.

The dependence of FAME content on the time of reaction and molar ratio is shown in Fig. 3.16. At lower value of molar ratio, FAME content is less even at higher time of reaction. As the molar ratio increased to 10:1, FAME content also increased with increase in time of reaction. However, the maximum FAME content is obtained at molar ratio of 10:1 and reaction time of 135mins.

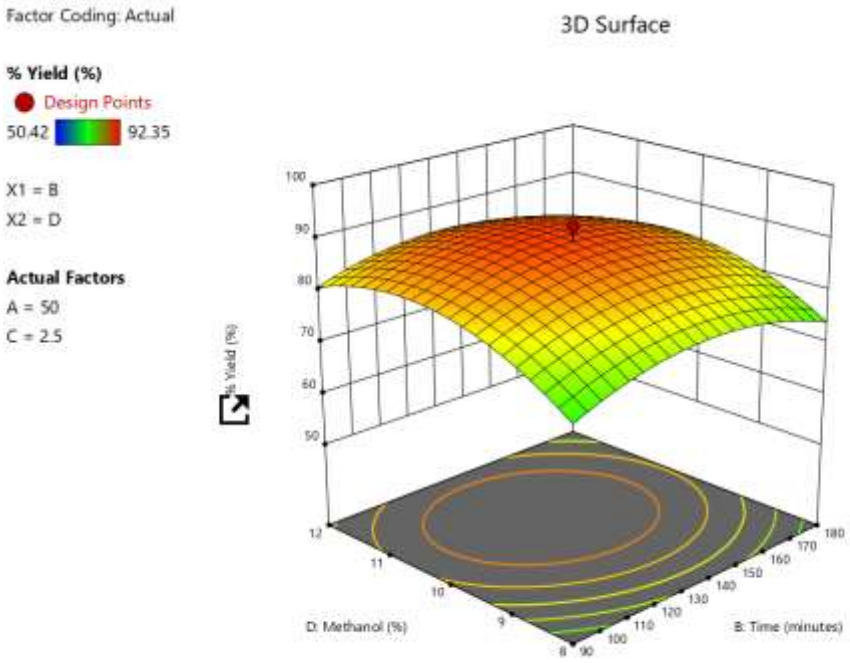

Figure 3.16: The surface interaction plot of time of reaction and methanol- oil ratio

The simultaneous dependence of FAME content on the molar ratio and catalyst concentration is shown in Fig. 3.17 while, the other two process parameters are maintained at their zero levels. At lower value of molar

© MAY 2026 | IRE Journals | Volume 9 Issue 11 | ISSN: 2456-8880
DOI: https://doi.org/10.64388/IREV9I11-1718212

ratio, FAME content is less even at higher catalyst concentration. As the molar ratio increased from to 10:1, FAME content also increased with increase in catalyst concentration. However, the maximum FAME content is obtained at molar ratio of 10:1 and catalyst concentration of 2.5%wt. Higher quantities beyond 10:1of methanol to oil molar ratio exhibits negative effect on FAME content, as it was clear by decreasing response with the increase in the molar ratio. This is because, at molar ratios of methanol/oil higher than 10:1, separation of esters from glycerol was problematic.

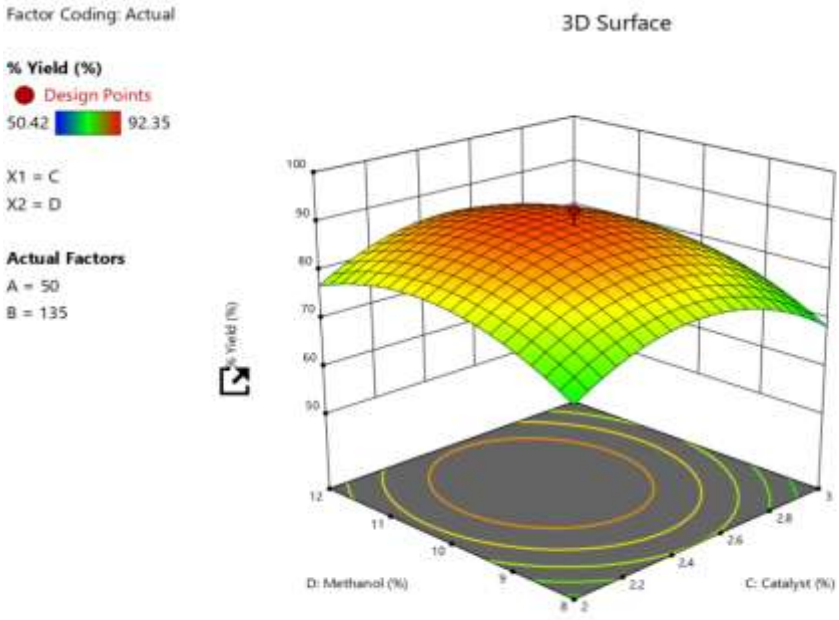

Figure 3.17: The surface interaction plot of catalyst concentration and methanol- oil ratio of FAME yield on African pear oil biodiesel.

3.7
Verification of RSM model for optimization of FAME yield at optimal conditions for Lard oil

The optimal values of the combination of four process parameters were estimated by solving the regression equation (Eq. 3.1) using Design Expert software. The optimum conditions obtained as follows: temperature (*A*) = 50ºC, time (B) = 135mins, catalyst (C) = 2.5%wt and methanol to oil molar ratio (D) = 10:1. For these optimum conditions, model predicted biodiesel FAME content of 94.987%. So, experimental runs were carried out three times in a flask under predicted conditions to validate the model as shown in table 3.12 below. Mean FAME content of 95.018% was obtained and shows the high degree of similarity between predicted and experimental values showing validity of RSM model.

Table 3.12: Verification of RSM model for optimization of FAME yield at optimal conditions for Lard oil FAME

Expt.	Time (mins)	Temp (ºC)	Catalyst (wt%)	Methanol/oil (wt%)		(%)	ExptPredict (%)	(%)	Error (%)
1	135.780	51.455	2.469	10.441	95.015	94.987	0.028		
2	135.780	51.455	2.469	10.441		95.021	94.987	0.034	
3	135.780	51.455	2.469	10.441		95.018	94.987	0.031	

3.8 Verification of RSM Model for Optimization of FAME Yield at Optimal Conditions for African Pear Oil Biodiesel

The optimal values of the combination of four process parameters were estimated by solving the regression equation (Eq. 3.2) using Design Expert software. The optimum conditions obtained as follows: temperature (*A*) = 50^{0}C, time (B) = 135mins, catalyst (C) = 2.5%wt and methanol to oil molar ratio (D) =10:1. For these optimum conditions, model predicted biodiesel FAME content of 89.976%. So, experimental runs were carried out three times in a flask under predicted

conditions to validate the model as shown in table 3.13 below. Mean FAME content of 90.005% was obtained and shows the high degree of similarity between predicted and experimental values showing validity of RSM model (*Ibiam et al.*, 2025).

Table 3.13: Verification of RSM model for optimization of FAME yield at optimal conditions for African pear oil

Expt. (mins)	Time (ºC)	Temp (wt%)	Catalyst (wt%)	Methanol/oil (%)	Expt (%)	Predict (%)	Error
1	133.338	51.481	2.464	10.489	90.010	89.976	0.034
2	133.338	51.481	2.464	10.489	89.996	89.976	0.020
3	133.338	51.481	2.464	10.489	90.008	89.976	0.032

3.9 Characterization of Biodiesel Produced at Optimal Condition

3.9.1 Physiochemical properties of the biodiesel

The biodiesel produced from both oil from Tables 3.7 and 3.8 corresponded with the ASTMD on Acid value, free fatty acid, Iodine value, specific gravity, density, viscosity, flash point, cloud point, pour point and cetane number. The acid value, FFA, moisture content, specific gravity, density and viscosity of the biodiesel produced from both the pig fat oil and African pear flesh oil from Table 3.14 when compared with their raw oil reduced significantly after the transesterification process. This showed that transesterification process actually took place leading to conversion of the raw oil to biodiesel. The viscosity of the African pear flesh biodiesel (1.6350 mm^2s^{-1}.) and pig fat biodiesel (1.5200mm^2s^{-1}) is low and fall within the ASTMD limit for a good biodiesel. Values of 4.14 and 4.54 mm2s-1, respectively at 40°C have been reported for animal fat and lard (Wörgetter *et al.*, 2006). The implication of the relatively low viscosity obtained in this work is that atomization of the biodiesel in the engine will be enhanced and the coking of the cylinders caused by highly viscous FAME may be averted by its use. The ASTM recommended viscosity range is 1.9 to 6.0 mm^2s^{-1} (National Standards for Biodiesel, 2009). The flash point of both the African pear flesh and pig fat biodiesel was high and falls within the standard limit as shown on Table 3.1.4. This implies that the biodiesels will be safer to handle since flash point is an important parameter that determines the safety, handling and storage of fuel. These properties imply that the biodiesel of African pear flesh and pig fat oil is promising.

The calculated cetane index of the pig fat methyl ester and African pear flesh methyl ester was 58.1 and 58.1 respectively. The ASTM standard for cetane index is ≥ 40. Cetane number increases with increase in the number of carbon atoms for saturated carboxylic acids. The presence of about 72% and 63% saturated fatty acids (palmitic, lauric, myristic and stearic) in African pear flesh and pig fat oils respectively may have led to the relatively high value of cetane index obtained since the unsaturated components are mainly monounsaturated, oleic and linoleic. Ikwuagwu *et al.* (2000) reported a cetane index value of 44.81 for rubber seed oil biodiesel.

Generally, biodiesel from more saturated feedstocks have higher cetane numbers and better oxidation stability but poor cold flow properties (Van Gerpen *et al.*, 2007). Either too high or too low a cetane number can cause operational problems (Knothe *et al.*, 1997). In the former case i.e when cetane number is too high, combustion can occur before the fuel and air are properly mixed resulting in incomplete combustion and smoke whereas in the latter case i.e when cetane number is too low, engine roughness, misfiring, higher air temperatures, slower engine warm-up and incomplete combustion occurs. The higher cetane index of the biodiesel means that its ignition temperature is good.

Table 3.14: Characterization of the biodiesel from Lard and African pear (Ube) oil compared with ASTMD6751-09.

Parameter	Lard oil diesel	pear oil diesel	ASTM
Moisture (%)	0.0341	0.0186	0.05 max
Acid value (mgKOH/g)	0.14	0.27	0-0.50
FFA (mgKOH/g)	0.07	0.14	0-0.5
Iodine value (gI_2/100g)	52.21	52.16	<125

Saponification Value (mgKOH/g)	249.13	224.34	-
Peroxide value (MEq/kg)	9.2	6.4	-
Specific gravity	0.8996	0.8479	0.86-0.90
Density(g/ml)	0.8393	0.8441	0.888minimum
Refractive index	1.4631	1.4635	-
Viscosity@ 40 (pa.s)	1.5200	1.6350	1.9-6.0
Viscosity@100 (pa.s)	1.3507	1.4272	-
Flash point(^{0}C)	145	152	130 minimum
Fire point(^{0}C)	156	158	
Cloud point(^{0}C)	10	11	-3 to 12
Pour point(^{0}C)	4	8	-15to 10
Cetane number	58.1	58.1	47 minimum
Sulphure	0.11	0.17	0.05 mxa
Sulphated Ash	0.0384	0.0399	0.02 max
Carbon Residue	0.093	0.077	0.05 max
Oxidation Stability	6h	5.6h	3h minimum

3.9.2 FTIR analysis of the biodiesel

Table 3.15 and 3.16 below is the interpretation table for biodiesel produced from the lard oil and African pear oil at optimal condition. The FTIR spectra of the raw oil and biodiesel have similar pattern because of few similarities that exist among triglycerides and methyl ester in their functional groups. However, small difference is observed in the following regions (CH_3andC–Oester) because biodiesel had a different functional group (CH_3) bonded compared to the raw pig fat oil and African pear flesh oil. In table 3.15 and 3.16, the strong ester peak at 1170–1300cm^1(C–Oester) are clearly present in the spectra (*Ibiam et al.*, 2025). Outside this region, another characteristic peak that indicates the presence of CH_3 group in the mixtures of methyl ester can be observed at 2990-2850cm^1.

Table 3.15: FTIR Interpretation of the Pig Fat (Lard) Oil Biodiesel

Peak value	Peak Intensity	Group and class	Bonds
3374.191	Strong	-OH in alcohols and phenols	OH Stretch
3108. 084	Medium or	=CH in aromatic and unsaturated hydrocarbons	=CH-H Stretch
	Very broad	-OH in carboxylic acids	H-bonded OH stretch
2873.946	Medium	-CH_3 attached to O or N	CH stretching modes
2472.515	Very broad	-OH in carboxylic acids	H-bonded OH stretch
2107.246	Medium	C≡N in thiocyanates	C≡N stretch
1651.049	Strong	NH_2 in amino acid	NH_2 deformation
1168.141	Strong	C-O in acids, esters	C-O stretch
667.3987	Strong	C-C-CHO in aldeydes	C-C-CHO bending

African pear flesh oil biodiesel. In table 3.16, the strong ester peak at 1170–1300cm^1(C–Oester) are clearly present in the spectra.

Outside this region, another characteristic peak that indicates the presence of CH_3 group in the mixtures of methyl ester can be observed at 2990-2850cm^1.

Table 3.16: FTIR interpretation of the African pear (Ube) Biodiesel

Peak value	Peak Intensity	Group and class	Bonds
3647.274	Strong	OH in alcohols and phenols	OH stretch

3327.07	Medium-strong	≡CH in acetylenes	≡CH stretc
3190.927	Medium or Very broad	=CH in aromatic and unsaturatedhydrocarbons -OH in carboxylic acids	=CH-H Stretch H-bonded OH stretch
2980.649	Medium-Strong	-CH_3 and CH_2 in aliphatic compounds	CH antisym and sym stretching
2787.625	Medium	-CH_3 attached to O or N	CH stretching modes
2564.897	Weak	SH in alkyl mercapton	SH stretch
2453.067	Very broad	OH in carboxylic acids	H-bonded OH stretch
2129.161	Medium	C≡N in thiocyanates	C≡N stretch
2210.092	Medium strong	C≡N in nitriles	C≡N stretch
1846.821	Strong	C=O in β-lactones	C=O stretch
1686.355	Strong	NH_2 in amino acid	NH_2 deformation
1308.579	Strong	NO_2 in aromatic nitro compounds	NO_2 antisym stretch
	Strong Medium-strong	NH_3^+ in amino acids or hydrochlorides N=N-O in azoxy compounds	NH_3^+ deformation N=N-O antisym stretch
855.3796	Very strong	1,2,4- trisubt. Benzene	CH out of plane deformation (two bands)
744.9324	Strong	0-disubst. Benzene	CH out of plane deformation

3.10 Kinetic Study of Biodiesel Production from African pear flesh and lard Oils

The data required for developing the kinetic model of the transesterification of African pear oil and lard oil was generated by conducting experiment of biodiesel production of lard and African pear oil using the optimal conditions of catalyst (2.5%wt) and methanol (10:1) at different reaction temperature of 40, 50 and 60^{o}C, and different reaction time of 30mins, 60mins, 90mins,120mins and 150mins. This reaction kinetic is a function of the concentration of oil (Triglyceride, TG) and reaction temperature. The stoichiometry of the transesterification process is given as follows:

$$TG + 3MeOH3 \longrightarrow RCOOCH_3 + Glycerol \quad (3.3)$$

To determine the rate of reaction per unit time, r, the following equation was used (Kansedo et al 2013).

$$r = dX/dt = k\,(K)\,(f\,x) \quad (3.4)$$

$$(f\,x) = (1 - X_A) \quad (3.5)$$

$$r = dx/dt = k(1 - X_A) \quad (3.6)$$

where X_A is the mole fraction of TG converted at time, t. Upon integration, the following equation is obtained:

$$-\ln(1-X_A) = K \quad (3.7)$$

The integration constant. K can be obtained by plotting -In (l-X_A) versus time, t.

Table 3.17: Determination of rate constant from transesterification process of African pear oil at 40^{0}C temperature and time 30, 60, 90, 120 and 150 minutes at constant optimum catalyst and methanol conditions of 2.5%wt and 10:1.

Time	%Yield(X_A)	(1- X_A)	-ln(1- X_A)
30	30.08	-29.08	3.3701
60	40.13	-39.13	3.6669
90	53.79	-52.79	3.9663
120	69.34	-68.34	4.2245
150	78.21	-77.21	4.3465

© MAY 2026 | IRE Journals | Volume 9 Issue 11 | ISSN: 2456-8880
DOI: https://doi.org/10.64388/IREV9I11-1718212

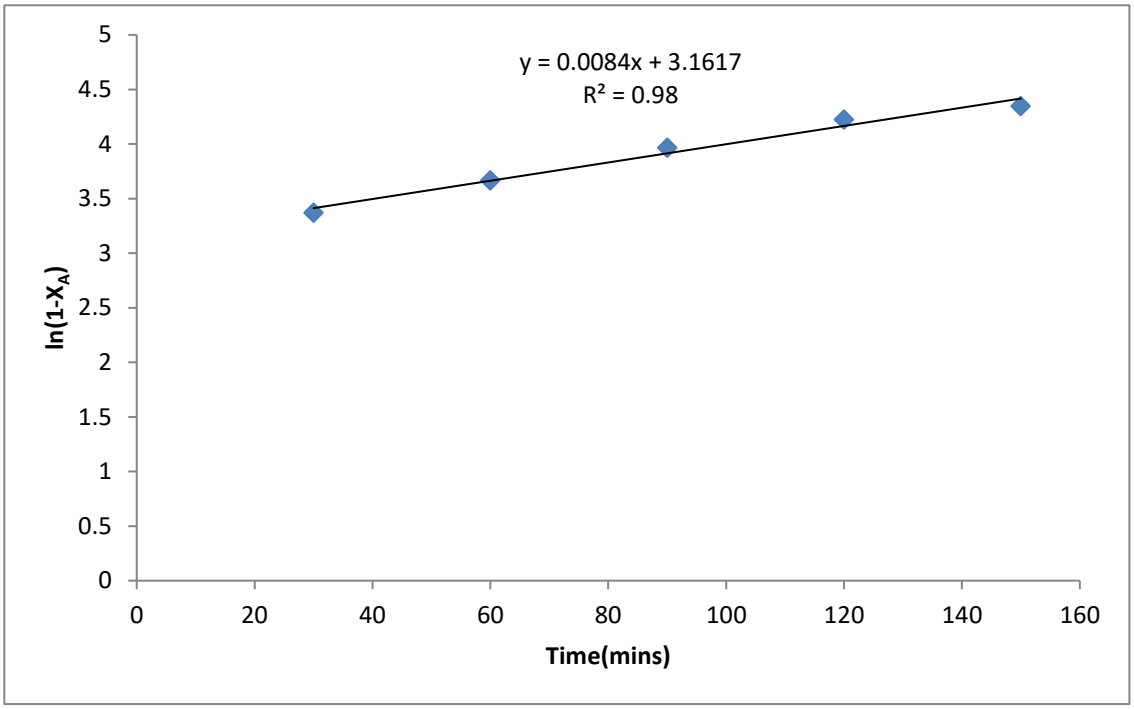

Figure 3.18: Showing dependence of ln(l-X_A) versus time, t during transesterification reaction with respect to temperature 40^{0}C, based on the catalyst concentration of 2.5 w% and methanol /oil weight: 10:1. X_A is the mole fraction of TG converted at time, t

Table 3.18: Determination of rate constant of transesterification process of African pear oil at 50^{0}C temperature time 30, 60, 90, 120 and 150 minutes at constant optimum catalyst and methanol conditions of 2.5%wt and 10:1.

Time	%Yield (X_A)	(1-X_A)	-ln(1-X_A)
30	50.47	-49.47	3.9014
60	60.36	-59.36	4.0836
90	70.57	-69.57	4.2423
120	78.87	-77.87	4.3550
150	85.30	-74.30	4.4462

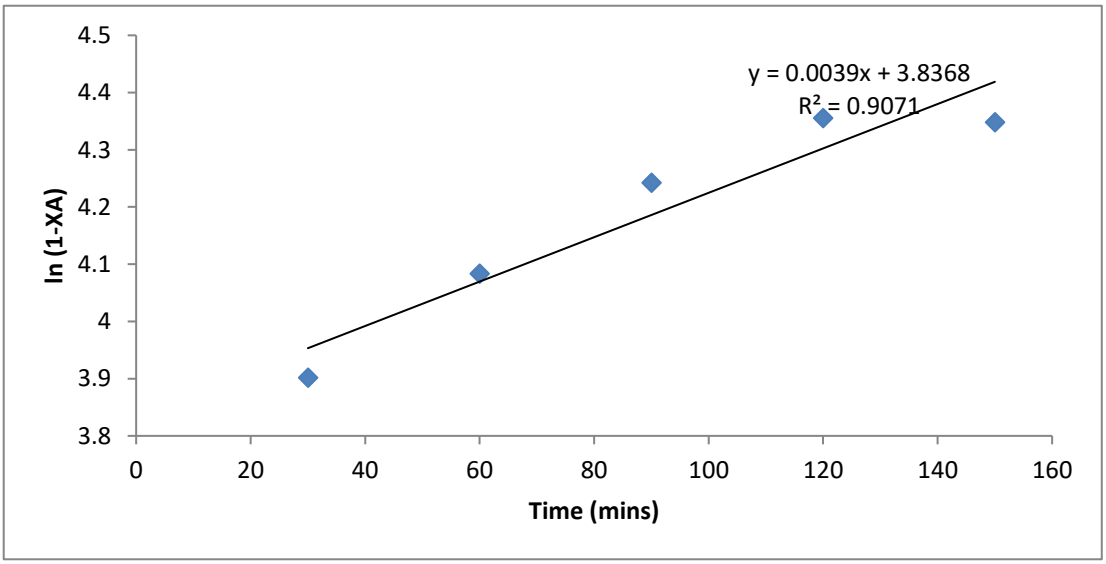

Figure 3.19: Dependence of ln(l-X_A) versus time, t during transesterification reaction with respect to temperature 50^{0}C, based on the catalyst concentration 2.5w% and methanol /oil weight: 10:1. X_A is the mole fraction of TG converted at time, t

© MAY 2026 | IRE Journals | Volume 9 Issue 11 | ISSN: 2456-8880
DOI: https://doi.org/10.64388/IREV9I11-1718212

Table 3.19: Determination of rate constant of transesterification process of African pear oil at 60°C temperature time 30, 60, 90, 120 and 150 minutes at constant optimum catalyst and methanol conditions of 2.5%wt and 10:1.

Time	%Yield (X_A)	($1-X_A$)	$-\ln(1-X_A)$
30	60.85	-59.85	4.0918
60	70.15	-69.15	4.2363
90	78.45	-77.45	4.3496
120	84.89	-83.89	4.4295
150	90.56	-89.56	4.4949

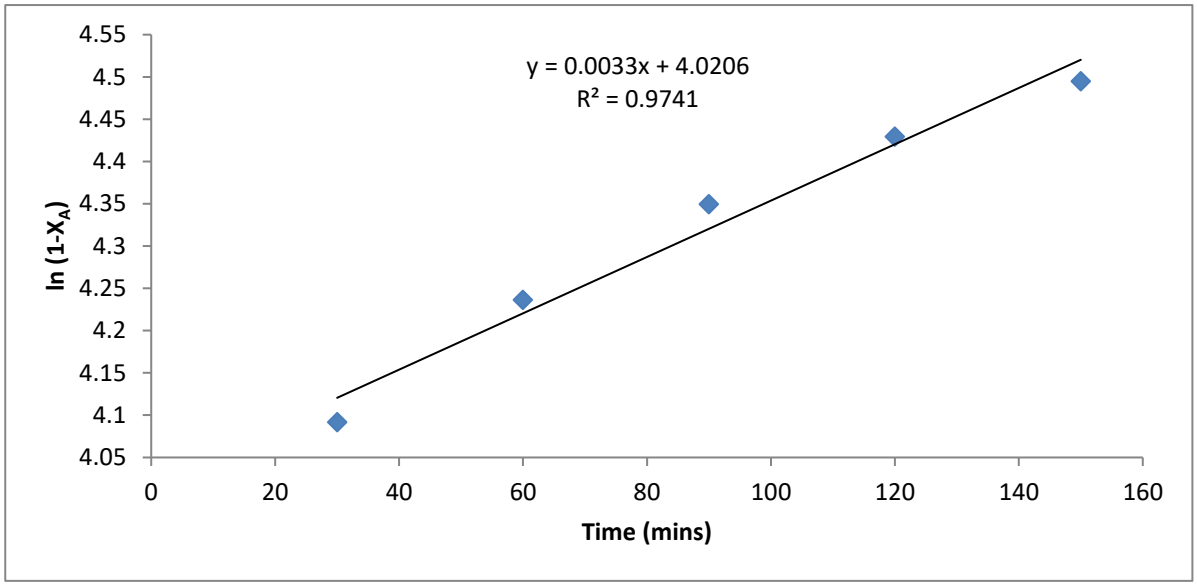

Figure 3.20: Dependence of $\ln(1-X_A)$ versus time, t during transesterification reaction with respect to temperature 60^0C, based on the catalyst concentration of 2.5w% and methanol /oil weight: 10:1. X_A is the mole fraction of TG converted at time, t

Table 3.20: Determination of rate constant of transesterification process of lard oil at 40^0C temperature and time interval of 30, 60, 90, 120 and 150 minutes at constant optimum catalyst and methanol conditions of 2.5%wt and 10:1.

Time	%Yield (X_A)	($1-X_A$)	$-\ln(1-X_A)$
30	48.79	-47.79	3.8668
60	52.447	-51.47	3.9602
90	64.69	-63.69	4.1540
120	76.45	-75.45	4.3235
150	80.59	-79.59	4.3769

© MAY 2026 | IRE Journals | Volume 9 Issue 11 | ISSN: 2456-8880
DOI: https://doi.org/10.64388/IREV9I11-1718212

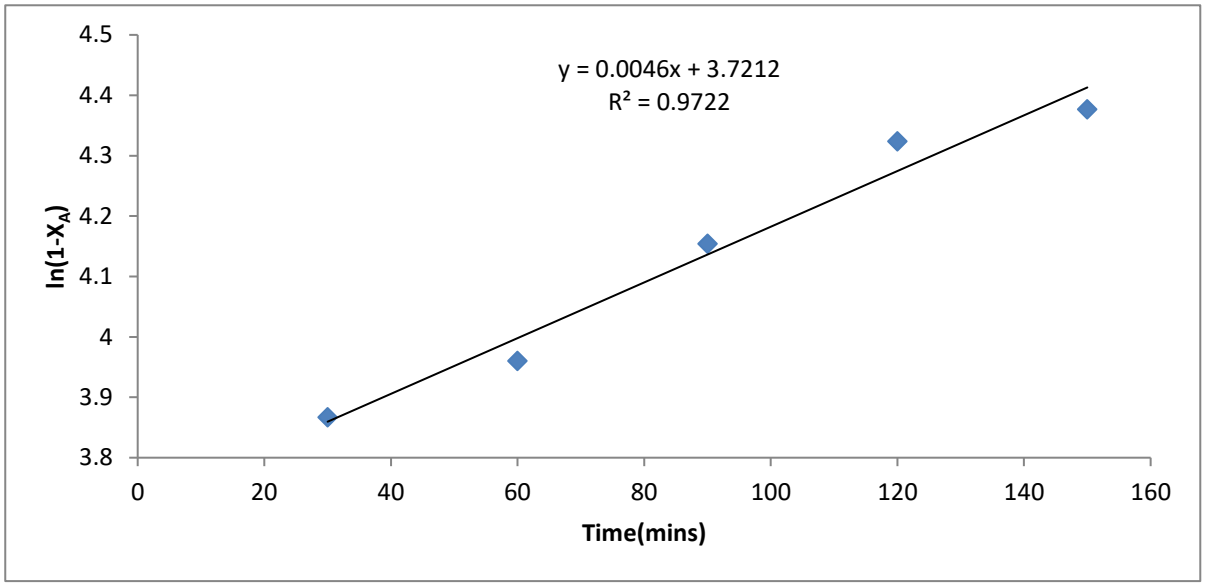

Figure 3.21: Dependence of ln(l-X_A) versus time, t during transesterification reaction with respect to temperature 40^{0}C, based on the catalyst concentration and of 2.5 w% and methanol /oil weight: 10:1. X_A is the mole fraction of TG converted at time, t

Table 3.21: Determination of rate constant of transesterification process of lard oil at 50^{0}C temperature time 30, 60, 90, 120 and 150 minutes at constant optimum catalyst and methanol conditions of 2.5%wt and 10:1.

Time	%Yield(X_A)	(1-X_A)	-ln(1-X_A)
30	57.81	-56.81	4.0397
60	65.94	-64.94	4.1735
90	76.45	-75.45	4.3235
120	84.69	-83.69	4.4271
150	87.32	-86.32	4.4581

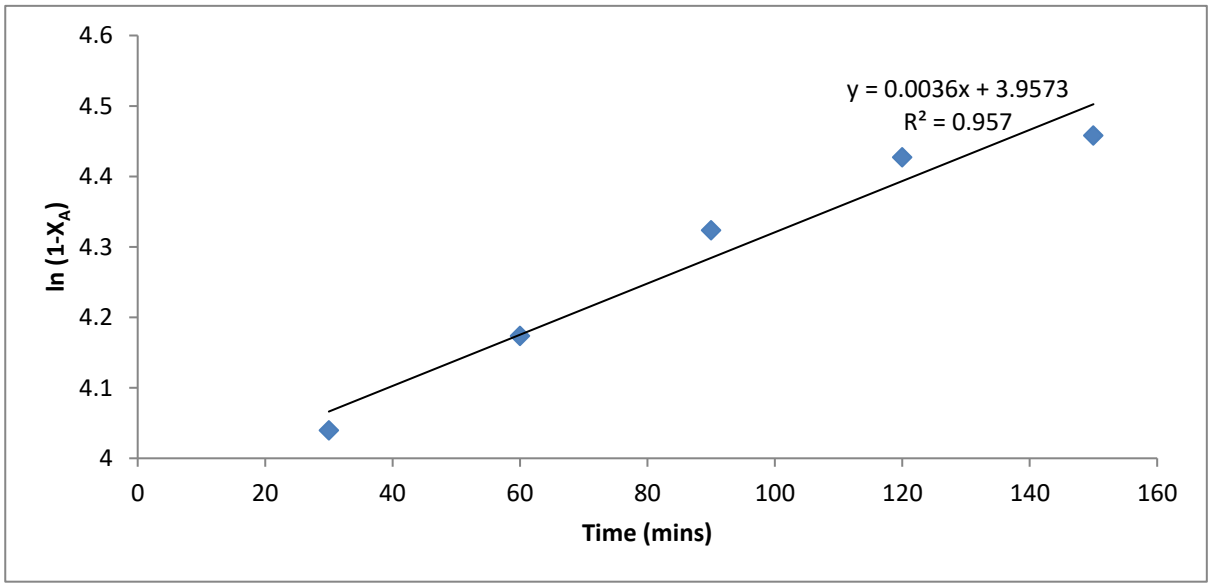

Figure 3.22: Dependence of ln(l-X_A) versus time, t during transesterification reaction with respect to temperature 50^{0}C, based on the catalyst concentration of 2.5w% and methanol /oil weight: 10:1. X_A is the mole fraction of TG converted at time, t

Table 3.22: The kinetic result of transesterification process of lard oil at 60^0C temperature and time 30, 60, 90, 120 and 150 minutes at constant optimum catalyst and methanol conditions of 2.5%wt and 10:1.

Time	%Yield (X_A)	($1-X_A$)	$-\ln(1-X_A)$
30	65.52	-64.52	4.1670
60	72.50	-71.50	4.2697
90	80.52	-79.52	4.3760
120	87.94	-86.94	4.4652
150	90.21	-89.21	4.4910

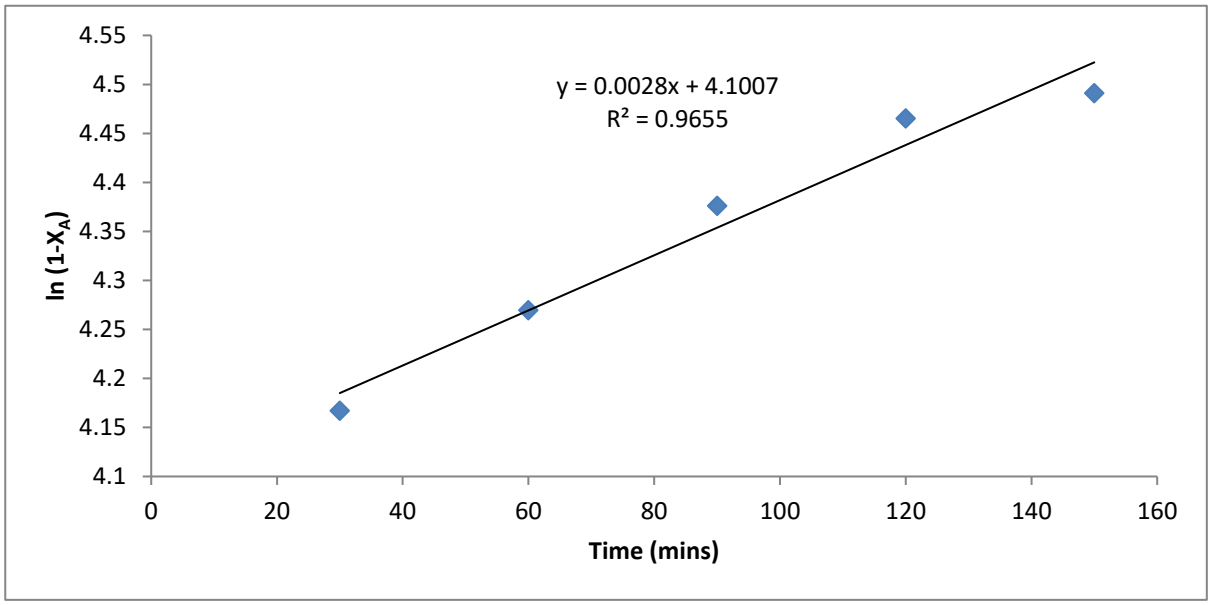

Figure 3.23: Dependence of $\ln(1-X_A)$ versus time, t during transesterification reaction with respect to temperature 60^0C, based on thecatalyst concentration of 2.5w% and methanol /oil weight: 10:1. X_A is the mole fraction of TG converted at time, t.

3.11 Thermodynamic Study of Transesterification Reaction of African Pear Flesh and Lard Oils

The influence of temperature on the global reaction rate constant was determined fitting k to the Arrhenius equation,

$$K(T) = k = A\, e^{(-Ea/RT)} \quad (3.8)$$

On integrating

$$\ln k = \ln A - (Ea/RT) \quad (3.9)$$

Where, A is the frequency factor in min^{-1}, Ea is activation energy in KJ $mole^{-1}$, R is universal ideal gas constant 8.314J/mole-K and T is temperature in K.

The activation energy was estimated by plotting lnk as a function of reciprocal temperature (1/T). Thus, the slope and the intercept of the plot would be equivalent to (-Ea/R) and ln A respectively. Figure 3.24 and Fig.3.25 showed the Arrhenius plot used to obtain the activation energy from the temperature dependence of the initial rates for the methanolysis of African pear oil and lard oil using calcinated cow bone as a catalyst. The activation energy and frequency factor for the transesterification reaction was calculated as 40.75KJ $mole^{-1}/8.6 \times 10^8/s^{-1}$ and 28.73KJ $mole^1/1.6 \times 10^7/s^{-1}$ for African pear oil and lard oil, respectively. These activation energies are slightly higher than those studies by different authors (Sivakumar, 2013, Freedman 1986, Morgenstern 2006). This may be due to the higher viscosity as well as the higher saturated fatty acid profile of Lard oil and African pear oil comparative with the other oils. Wang and Briggs, (2002) reported that higher activation energy value indicated a more rapid change in viscosity with temperature. This is because of higher saturated fatty acids composition present in oil. The similar trend is observed in our case. The positive value of the activation energy indicates endothermic reactions, whereby energy (heat) is required for the reactions to take place. The activation energy, enthalpy change, entropy change and Gibbs free energy change for both African pear flesh oil and lard oil was determined from the plot of lnK versus 1/T respectively in figure 3.24 and 3.25. The enthalpy and entropy changes of the process for the both African pear flesh oil and lard oil

© MAY 2026 | IRE Journals | Volume 9 Issue 11 | ISSN: 2456-8880
DOI: https://doi.org/10.64388/IREV9I11-1718212

are both positive as shown from the plot of $\ln Y_T$ versus 1/T, meaning that the reaction is endothermic, because the reaction mixture was heated in order to turn into product. Entropy S is a state function and is a measure of disorder or randomness whereas entropy change shows whether the system can be returned to the initial state or not after the completion of the process. Here, the positive value of entropy change ($\Delta S > 0$) demonstrates that the process is a non-spontaneous reversible reaction. Free energy illustrates the energy profile of the system. From the experimental observation, the negative value of ΔG confirms that the process requires higher energy state. Hence, the transesterification process of the both oil samples is non-spontaneous (endergonic) reaction.

With the kinetics parameters obtained, a mathematical model was proposed for the base catalyzed transesterification of African pear oil and lard oil as Eq. (10) and Eq. (11) respectively.

$$r = dx/dt = 8.6 \times 10^8 \, e^{(-40.75/RT)} \quad (3.10)$$

$$r = dx/dt = 1.6 \times 10^7 \, e^{(-28.73/RT)} \quad (3.11)$$

The goodness of fit of the proposed model was determined by predicting the conversion at temperature of 338 K and at different reaction times. Comparison with the actual (experimental) vs. predicted conversion at the same reaction temperature was made to determine the errors between the predicted and the actual values. Eq. (10) and Eq. (11) were plotted using Excel whereby the data for the actual curve was obtained experimentally. Figure 3.26 and Fig.3.27 shows the comparison between the actual and predicted conversion at different times. From Fig. 3.26 and Fig. 3.27, the error between the predicted and experimental conversion obtained by the proposed models, were less than 10%. This shows that the models developed (model from ANOVA and kinetics model) are highly reliable in representing the whole experimental data and also accurate in predicting the kinetics of the base catalyzed transesterification of African pear oil and lard oil.

Table 3.23: The thermodynamic result of transesterification process of African pear flesh oil at different temperature of 40ºC,50ºC, and 60ºC.

T	K	Ink	1/T	R^2
313	0.008	-4.8283	0.0032	0.980
323	0.003	-5.8091	0.0031	0.980
333	0.003	-5.8091	0.0030	0.974

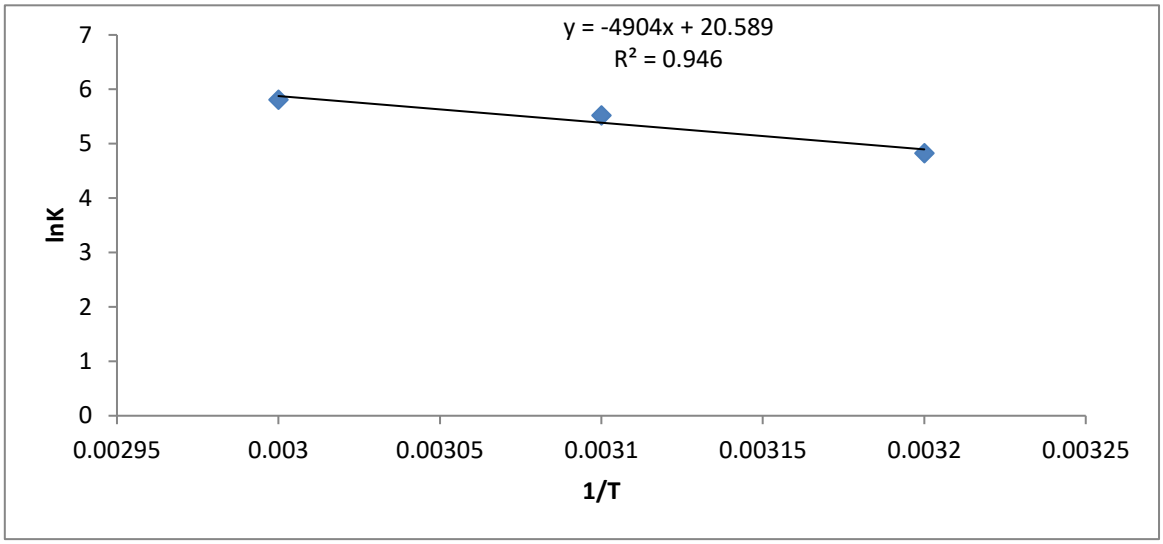

Figure 3.24: Dependence of lnk versus 1/T during transesterification reaction of African pear flesh oil with respect to different temperature conditions.

Table 3.24: The thermodynamic result of transesterification process of lard oil at different temperature of 40^0c, 50^0c,and 60^0c.

T	k	Ink	1/T	R^2
313	0.004	-5.5215	0.0032	0.972
323	0.003	-5.8091	0.0031	0.957

© MAY 2026 | IRE Journals | Volume 9 Issue 11 | ISSN: 2456-8880
DOI: https://doi.org/10.64388/IREV9I11-1718212

333	0.002	-6.2146	0.0030	0.965

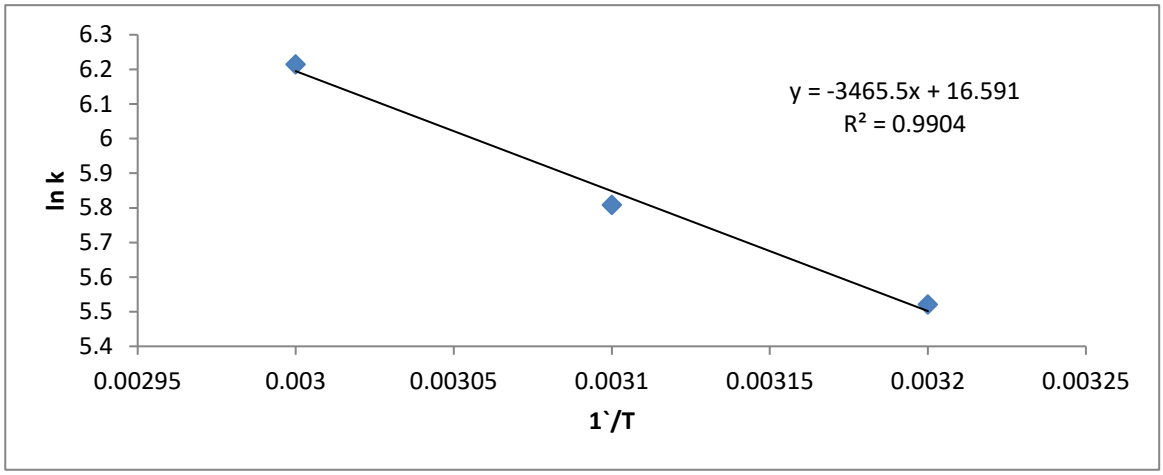

Figure 3.25: Dependence of lnk versus 1/T during transesterification reaction of lard oil with respect to different temperature conditions.

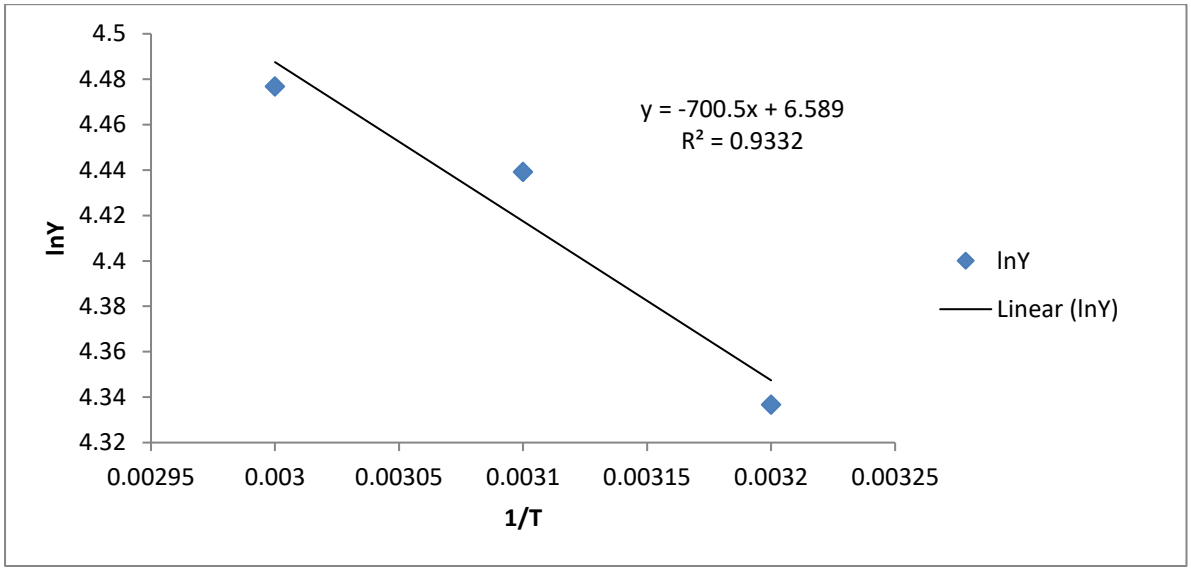

Figure 3.26: Plot of $\ln Y_T$ versus 1/T for thermodynamic parameters of lard oil

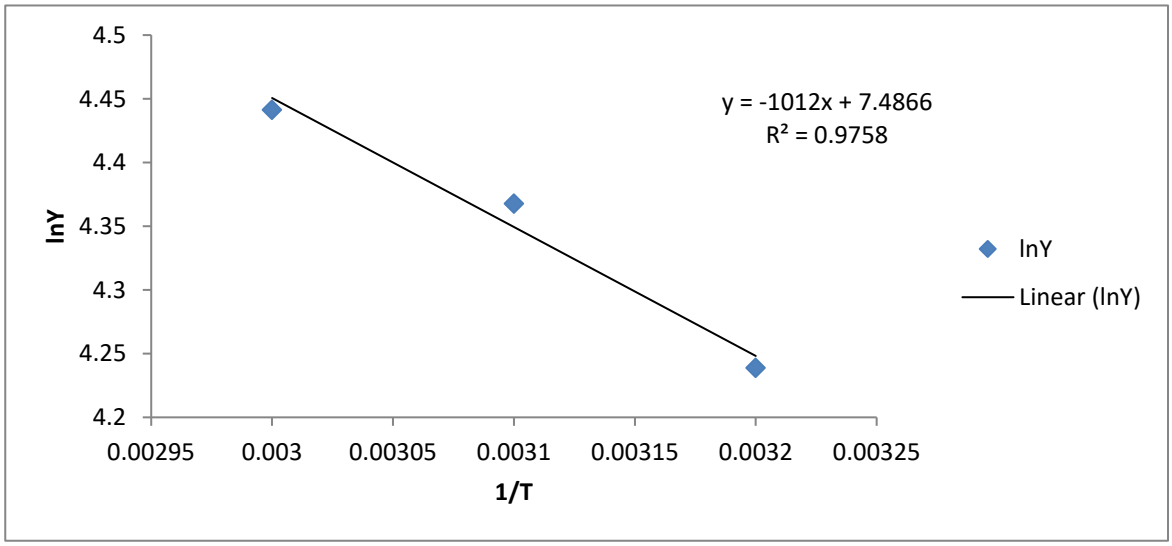

Figure 3.27: Plot of $\ln Y_T$ versus 1/T for thermodynamic parameters of African pear oil

© MAY 2026 | IRE Journals | Volume 9 Issue 11 | ISSN: 2456-8880
DOI: https://doi.org/10.64388/IREV9I11-1718212

Table 3.25: Influence of each temperature in kinetic and thermodynamic parameters of biodiesel esterification process.

		Lard oil	African pear oil
Ea / KJ mol^{-1}	28.73	40.75	
ΔH / KJ mol^{-1}	5.82	8.41	
ΔS / KJ mol^{-1}	54.78	62.24	
ΔG / KJ mol^{-1}	-48.96		-53.83

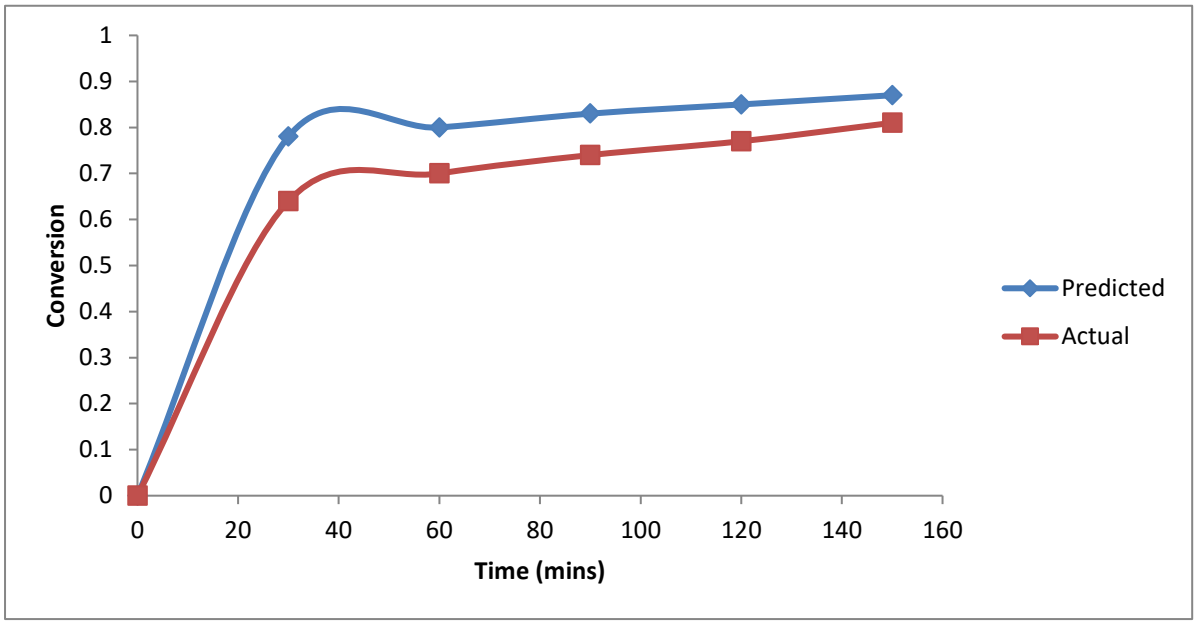

Figure 3.28: Plot of predicted vs actual conversion rate using the proposed model equation for African pear oil at temperature of 338 with different timing.

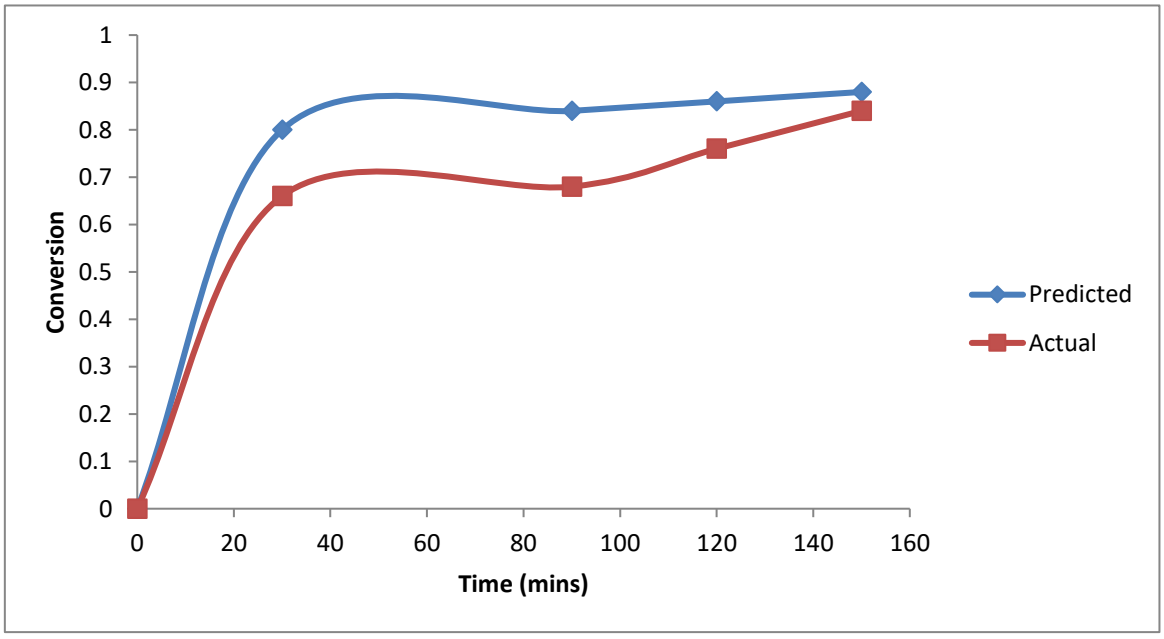

Figure 3.29: Plot of predicted vs actual conversion rate using the proposed model equation for Lard oil at temperature of 338 with different timing.

IV. CONCLUSION

This study was carried out to produce biodiesel from African pear and lard oil by heterogeneous base-catalyzed transesterification and determining its characteristics. This research was conducted by using African pear oil and Lard oil as raw material, methanol as alcohol and calcinated cow bone as source of CaO as a base heterogeneous catalyst. The alkali transesterification process was performed. Four parameters taken into consideration: methanol/oil ratio, temperature, catalyst concentration and time. The optimum biodiesel yield from the research was 95.02% and 90.01% for Lard oil and African pear oil respectively at methanol: oil ratio of 10:1, reaction, temperature of 50 ^{0}C, contact time of 135mins and catalyst concentration of 2.5 %wt. And, the physical characteristics obtained from the final optimum biodiesel yield were within ASTM D 6751 and European Standards EN 14214.

REFERENCES

[1] Abdoulmoumine, N. (2010). Sulphated and Hydroxide Supported on Zirconium Oxide Catalyst for Biodiesel Production. Published M.Sc thesis.Faculty of the Virginia Polytechnic Institute and State University, USA.

[2] Adebayo GB, Ameen OM, Abass LT (2011). Physico-chemical properties of biodiesel produced from Jatropha curcas oil and fossil diesel. J. Microbiol. Biotech. Res. 1(1): 12-16.

[3] Agadale, S. S.; Jugulkar, L. M. (2012) Review of VariousReaction Parameters and Other Factors Affecting onProduction of Chicken Fat Based Biodiesel, *InternationalJournal of Modern Engineering Research*, 2(2), 407-411.

[4] Agarwal Madhu and Garima Chauhan (2011). Heterogeneous catalysis for Biodiesel Production: Review. International Conference on renewable energy.

[5] Akinwekomi, A.D. Omotoyinbo, J.A. and Folorunso, D. (2012). Effect of High Alumina Cement on Selected Foundry Properties of Anthill Clay.*Leonardo Electronic Journal of Practices and Technology*, 1, 37-46.

[6] Alba-Rubio, A.C. Santamaría-González, J. Mérida-Robles, J. M. Moreno-Tost, R. Martin Alonso, D. Jiménez-López, A. and Maireles-Torres, P. (2010). Hetergeneous Transesterification Processes by Using CaO Supported on Zinc Oxide as Basic Catalysts. *Catalysis. Today*, 149 (3-4), 281-287.

[7] Al-Widyan ML, Al-Shyoukh AO (2002). Experimental evaluation of the transesterification of waste palm oil into biodiesel.Bioresour. Technol. 85(3): 253-256.

[8] Anitha, A.; Dawn, S.S. (2010) Performance Characteristicsof Biodiesel Produced from Waste Groundnut Oil usingSupported Heteropolyacids. *International Journal of Chemical Engineering and Applications*, 1(3), 261-265.

[9] Arai, M. and Zhao, F. (2015). Metal Catalysts Recycling and Heterogeneous/Homogeneous Catalysis.*Catalysis*, 5, 868-870.

[10] Azam, M.M., Waris, A., Nahar, N.M., 2005.Prospects and potential of fatty acidmethyl esters of some non-traditional seed oils for use as biodiesel in India. Biomass Bioenergy 29, 293–302.

[11] Azjargal Janchiva, Youngtaig Oh, Seunghun Choi. High quality biodiesel production from pork lard by high solvent additive. Research article doi: 10.2306/scienceasia1513-1874.2012.38.095

[12] Babcock RE, Clausen EC, Popp M, Mattingly B (2007). BiodieselProduction from Varying Grades of Beef Tallow and Chicken Fat.Final Report, Award No. MBTC-2058. Mark Blackwell TransportationCentre pp. 1-12. Available at: http://hdl.handle.net/123456789/6980.

[13] Bankovic-llic I. B.; Stojkovic, I. J.; Stamenkovic, O. S; Velijkovic, V. B; Hung, Y. T. (2014). Waste Animal Fats as Feedstocks for Biodiesel Production. Civil and Environmental Engineering Faculty Publication, 104.

[14] Berrios M, Guti´errez MC, Mart´ın MA, Mart´ın A (2009) Application of the factorial design of experiments to biodiesel production from lard. Fuel Process Tech 90, 1447–51.

[15] Bhatti, H. N., Hanif, M. A., Qasim, M., & Rehman, A. U. (2008). Biodiesel production from waste tallow.*Fuel,* Vol.87, N.13-14, (October 2008), pp.2961–2966, ISSN 0016-2361

[16] Birla, A. Singh, B. Upadhyay, S.N. and Sharma, Y.C. (2012). Kinetics Studies of Synthesis of Biodiesel from Waste Frying Oil Using a Heterogeneous Catalyst Derived from Snail Shell. *Bioresource Technology.* 106, 95-100.

[17] Boey, P.L. Mariam, G.P., Hamid, S.A. and Ali, D.M.H. (2011). Utilization of Waste Cockle Shell (Anadara Granosa) in Biodiesel Production from Palm Olein Optimization Using Response Surface Methodology. *Fuel*, 90, 2353-2358.

[18] BS EN 590:2009 (2009), *Automotive fuels. diesel. Requirements and test methods*, London, Great Britain: BSI-British Standard Institution. Improvement on Fossil Diesel Quality (punchng.com/nnpc-produce diesel-corps)

[19] Canakci, M. and Sanli, H. (2008). Biodiesel Production from Various Feedstocks and Their Effects on the Fuel Properties.*Journal of Industrial Microbiology and Biotechnol*ogy, 35(5), 431-441.

[20] Chakraborty, R. Bepari, S. and Banerge, A. (2011). Application of Calcined Waste Fish Scale as Low-Cost Heterogeneous Catalyst for Biodiesel Synthesis.*Bioresource Technology*, 102, 3610-3618.

[21] Charoenchaitrakool M, Thienmethangkoon J (2011) Statistical optimization for biodiesel production from waste frying oil through two-step catalyzed process. Fuel Process Tech 92, 112–8.

[22] Chen X, Du W, Liu D (2008) Response surface optimization of biocatalytic biodiesel production with acid oil. Biochem Eng J 40, 423–9.

[23] Cho, Y.B. and Seo, G. (2010). High Activity of Acid Treated of Quail Eggshell Catalysts in the Transesterification of Palm Oil with Methanol. *Bioresource Technology*, 101: 8515 -8524.

[24] Chung KH, Kim J, Lee KY (2009). Biodiesel Production byTransesterification of Duck Tallow with Methanol on Alkali Catalysts.Biomass Bioenergy 33(1):155-158.

[25] Crymble SD, Hernandez R, French T, Zappi ME, Baldwin BS, ThomasD (2006). Kinetic Study of Biodiesel Production from Chinese TallowTree Oil, Poster Session: Catalysis and Reaction EngineeringDivision, AIChE Annual Meeting, San Francisco, CA, Nov. 15. No.416.

[26] Dai, Y. Chen, K. Wang, Y. and Chen, C. (2014). Application of Peanut Husk Ash as a Low-Cost Solid Catalyst for Biodiesel Production.*International Journal of Chemical Engineering and Applications*, 5(3), 276-280.

[27] Demirbas, A. (2005). Biodiesel production from vegetable oils via catalytic and non-catalytic supercritical methanol transesterification methods. Progress in Energy and Combustion Science, 31 (5-6), 466-487.

[28] Department of Chemical Engineering. In Alptekin, et al. (2011). World Ren. Energy Congress, 8-13 May, Sweden pp. 319- 326.

[29] Dev Anand1 M., Vijay Ananth S., Jackson D. and Prabhu N. Investigation of Biodiesel Production from High Free Fatty Acid through RSM Indian Journal of Science and Technology, Vol 9(13), DOI: 10.17485/ijst/2016/v9i13/90575, April 2016

[30] Dias J.M, Alvim-Ferraz M.C.M, Almeida M.F, "Comparison of the performance of different homogeneous alkali catalysts during transesterification of waste and virgin oils and evaluation of biodiesel quality," *Fuel* DOI 10.1016/j.fuel.2008.06.014, 2008.

[31] Dias J.M, Alvim-Ferraz MCM, Almeida MF (2009) Production of biodiesel from acid waste lard.Bioresource Tech 100, 6355–61.

[32] Ding, J. Xia, Z. and Lu, J. (2012). Esterification and Acidification of Waste Cooking Oil (Tan 68.81 mgKOH/g) for Biodiesel Production. *Energies*, 5, 2683-2691.

[33] Dossin, T.F., Reyniers, M.F., Berger, R.J., Marin, G.B., 2006. Simulation of heterogeneously MgO-catalyzed transesterification for fine-chemical and biodiesel industrial production.Appl. Catal. B: Gen. 67, 136–148.

[34] Dubois, P. Pollet, E. and Delcourt, C. and Alexandre, M. (2006).Transesterification Catalysts to Improve Clay Exfoliation in Synthetic Biodegradable Polyester Nanocomposites, *European Polymer Journal,* 42, 1330-1341.

[35] Ejikeme PM (2008). Fuel Properties of the Derivatives of Soybean Oil.J. Chem. Soc. Niger. 33(1):145-149.

[36] Encinar, J. M.; Gonzalez, J. F.; Rodriguez-Reinares, A., (2005). Biodiesel from used frying oil.Variables affecting the yields and characteristics of the biodiesel. Ind. Eng. Chem. Res., 44 (15), 5491-5499.

[37] Endalew, A.K. Kiros, Y. and Zanzi, R. (2011). Inorganic Heterogeneous Catalysts for Biodiesel Production from Vegetable Oils.*Biomass and Bioenergy*, 35, 3787-3809.

[38] Freedman, B.; Butterfield, R. O.; Pryde, E. H. Transesterification kinetics of soybean oil. *J. Am. Chem.Soc.* 63, 1375-1380□1986□.

[39] Fukuda, H. Kondo, A. and Noda, H. (2001). Biodiesel Fuel Production by Transesterification

of Oils.*Journal of Bioscience and Bioengineering*, 92(5), 405-416.

[40] Furuta, S. Matsuhashi, H. and Arata, K. (2004). Biodiesel Fuel Production with Solid Super Acid Catalysis in Fixed Bed Reactor Under Atmospheric Pressure. *Catalysis Communication*, 5(12), 712-723.

[41] Furuta, S. Matsuhashi, H. and Arata, K. (2006). Biodiesel Fuel Production with Solid Amorphouszirconia Catalysis in Fixed Bed Reactor.*Biomass & Bioenergy*, 30(10), 870-873.

[42] Garlapati, V.K.; Kant, R.; Kumari, A.; Mahapatra, P.; Das, P.; Banerjee, R. (2013) Lipase mediated transesterification of Simarouba glauca oil: a new feedstock for biodiesel production. *Sustainable Chemical Processes*, 2013, 1(11), 1-

[43] Geise, R. (2002). Biodiesel's Bright Future Deserves Equality. *Render Magazine*, Vol. 31, p.p. 16–17, ISSN 0090-8932

[44] Ghiaci, M. Aghabarari, B. and Gil, A. (2011).Production of Biodiesel by Transesterification of Natural Fatty Acids over Modified Organoclay Catalysts.*Fuel*, 90, 3382-3389.

[45] Goodrum JW, Geller DP, Adams TT (2003). Rhelogical Characterizationof Animal Fats and Their Mixtures with #2 Fuel Oil. Bio. Bioenergy 24(3):249-256.

[46] Gürü, M., Artukoglu, B. D., Keskin, A., & Koca, A. (2009). Biodiesel production from waste animal fat and improvement of its characteristics by synthesized nickel andmagnesium additive.*Energy Conversion and Management* Vol.50, No.3, (March2009), pp. 498-502, ISSN 0196-8904

[47] Harvey, A.P., Mackley, M.R., & Seliger, T. (2003). Process Intensification of Biodiesel Production Using a Continuous Oscillatory Flow Reactor.*Journal of Chemical Technology & Biotechnology,* Vol. 78, No. 2-3, (February - March 2003) p.p. 338–341. ISSN 0268-2575

[48] Hassani, M. Najafpour, G.D. Mohammadi, M. and Rabiee, M. (2014). Preparation, Characterization and Application of Zeolite-Based Catalyst for Production of Biodiesel from Waste Cooking Oil.*Journal of Scientific & Industrial Research*, 73, 129-133.

[49] Henne, G.A. (2009). Anthill as a Resource for Ceramics.Published PhD Thesis, Faculty of fine art, Kwame Nkrumah University of Science and Technology, Ghana. Hossain A.B and A.N. Boyce, Agricultural Science, vol. 15, no. 4, (2009), pp. 312-317.

[50] Heydarzadeh, J.K. Amini, G. Khalizadeh, M.A. Pazouki, M. Ghoreyshi, A.A. Rabeai M. and Najafpour, G.D. (2010). Esterification of Free Fatty Acids by Heterogeneous □-Alumina-Zirconia Catalysts for Biodiesel Synthesis.*World Applied Sciences Journal,* 9(11), 1306-1312.

[51] Highina, B.K.; Bugaje, I.M.; Umar, B. (2012) BiodieselProduction from Jatropha Caucus Oil in a Batch ReactorUsing Zinc Oxide as Catalyst, *Journal of Applied Phytotechnology in Environmental Sanitation*, 1(2), 61-66.

[52] Hogue, M. E.; Singh A, Chuan Yi, Biodiesel from lowcost feedstocks: the effects of process parameters on the biodiesel yield. Biomass Bioenergy, 2011: 35:1532-7

[53] Huang Y, Zheng H, Yan Y (2010) Optimization of lipase-catalyzed transesterification of lard for biodiesel production using response surface methodology. Appl Biochem Biotechnol 160, 504–15.

[54] Ibiam Prince Amauche, Amadi Chiubeze, Ezeamama Lilian, Ain Grace, Ifegbo Arinze N. (July 2022) Comparative Study of Phytochemical Properties of Some Bio-Material (African Yam Bean, Pigeon Pea, Pawpaw Leaf Powder, Moringa Seed and Pawpaw Seed) Am. J. Environ Econ. 1(1) 13-18

[55] Ibiam Prince Amauche. 9 MAR (2025) Synthesis of Eco-Frienmoly Biolubricant By Chemical Modificantion of Sandbox Seed Oil. IRE Journals. Volume 8. ISSN: 2456-8880

[56] Ibiam Prince Amauche, Jonah Chukwu Umeuzuegbu, Joseph Okechukwu Ezeugo, Okafor Blessing Onyinye (2025) Comparative evaluation of bioethanol production from cassava mill effluent and cassava peels using Zymomonas mobilis. World News of Natural Sciences 61(1), 1-56.

[57] Ibiam Prince Amauche, Udonne Joseph, Jeremiah S. H, and Ezeamama Lilian, (May, 2022) Performance Evaluation and Optimization of a Two Horse Power Concentric Tube Heat Exchanger, 22(7): 28-38, 2022; Article no. JERR.78268, ISSN: 2582-2926.

[58] Jeong G., H. Yang, D. Park, Optimization of transesterification of animal fat acid methyl ester using response surface methodology, Bioresour. Technol. 100 (1) (2009) 25–30

[59] Jitputti, J. Kitiyanan, B. Rangsunvigit, P. Bunyakiat, K. Attanatho, L. and

Jenvanitpanjakul, P. (2006) Transesterification of Crude Palm Kernel Oil and Crude Coconut Oil by Different Solid Catalysts.*Chemical Engineering Journal*. 116, 61-66.

[60] Kafuku, G. Lam, K.T. Kanselo, J. Lee, K.T. and Mbarawa, M. (2010). Heterogeneous Catalyzed Biodiesel Production from Moringa Oleifera Oil.*Fuel Processing Technology*, 91(11), 1525-1529.

[61] Kallo, D. (2001). Application of Natural Zeolites in Water and Wastewater Treatment. Mineralogical Society of America and Geochemical Society (Washington, DC).45, 519-550.

[62] Kamath HV, Regupathi I, Saidutta MB (2011) Optimization of two step karanja biodiesel synthesis under microwave irradiation. Fuel Process Tech 92, 100–5.

[63] Kansedo, J. B. (2009) Synthesis of Biodiesel from Palm Oiland Sea Mango Oil Using Sulfated Zirconia Catalyst. Mscthesis, Universiti Sains Malaysia.

[64] Kawashima, A. Matsubara, K. and Honda, K. (2008). Development of Heterogeneous Base Catalysts for Biodiesel Production.*Bioresource Technology*, 99 (9), 3439-3443.

[65] Knothe, G. (2006). Analyzing Biodiesel: Standards and Other Methods.*Journal of the American Oil Chemists' Society*, 83(10), 823-833.

[66] Kouzu, M. Kasuno, T. Tajika, M. Sugimoto, Y. Yamanaka, S. and Hidaka, J. (2008). Calcium Oxide as a Base Catalyst for Transesterification of Soybean Oil and its Application to Biodiesel Production.*Fuel*, 87, 2798-2806.

[67] Kristiansen, S.M. and Amelung, W. (2001). Abandoned Anthill in a Temperate Deciduous Forest Morphology and Organic Matter Composition.*European Journal of Soil Science*, 52, 355– 363.

[68] Lakhya, J.K. Singh, C. Jutika, B. Rupam, K. and Dhanapati, D. (2012). Biochar Supported CaO as Heterogeneous Catalyst for Biodiesel Production. *International Journal of Innovative Research & Development*, 1(7), 186-195.

[69] Lam, M.K. and Lee, K.T. (2011). Mixed Methanol-Ethanol Technology to Produce Greener Biodiesel from Waste Cooking Oil: A Breakthrough for SO2-4/SnO2-SiO2 Catalyst. *Fuel Processing Technology,* 92, 1639-1645.

[70] Lee, K. T.; Foglia, T. A.; Chang, K. S., (2002).Productionof alkyl ester as biodiesel from fractionated lard andrestaurant grease. J. Am. Oil Chem. Soc., 79 (2), 191-195.

[71] Li, H., Xie, W., 2006. Transesterification of soybean oil to biodiesel with Zn/I2 catalyst. Catal.Lett. 107, 25–30

[72] Lopez, D.E. Godwin Jr. J.G. Bruce, O.A. and Lotero, E. (2005).Transesterification of Triacetin with Alcohol on Solid Acid and Base Catalysts. *Applied Catalysis A: General*, 2, 97-105.

[73] Lu J, Nie K, Xie F, Wang F, Tan T (2007) Enzymatic synthesis of fatty acid methyl esters from lard with immobilized Candida sp. 99-125. Process Biochem 42,1367–70..

[74] M. A. Mujeeb, A. B. Vedamurthy and Shivashargna, C. T., A Review Current strategies and prospects of biodiesel production; Department of Biotechnology and Microbiology, Karnatak university, Dharwad, India

[75] Ma, F. and Hanna, M.A. (1999). Biodiesel Production: a Review. *Bioresource Technology,* 70,1-15.

[76] Macêdo, C.C.S. Abreu, F.R. Tavares, A.P. Alves, M.B. Zara, L.F. Rubim, J.C. and Suarez, P.A.Z. (2006). New Heterogeneous Metal-Oxides Based Catalyst for Vegetable Oil Transesterification. *Journal of Brazilian Chemical Society*, 17 (7), 1291-1296.

[77] MacLeod, C. S., Harvey, A. P., Lee, A. F., & Wilson, K. (2008).Evaluation of the activity and stability of alkali-doped metal oxide catalysts for application to an intensified method of biodiesel production. *Chemical Engineering Journal*, Vol. 135, No. 1-2,(January 2008), p.p. 63-70, ISSN 1385-8947

[78] Man, L.F. (2013). Synthesis and Characterization of Solid Metal Oxide Nanostructure for Biodiesel Production. The HKU Scholar Hub, University of Hong Kong.

[79] Marchetti, J. M.; Miguel, V. U.; Errazu, A. F., (2008).Technoeconomic study of different alternatives for biodiesel production. Fuel Process Tech., 89 (8), 740-748. Mattingly B (2005).Production of Biodiesel from Chicken Fat Containing Free Fatty Acids.

[80] Mattingly B, Manning P, Voon J, Himstedt H, Clausen E, Popp M, Babcock R (2004). Comparative Esterification of Agricultural Oils for Biodiesel Blending. Final Report, Award No.MBTC-2052. Mark Blackwell Transportation Centre. Available

at:http://www.markblackwell.org/research/finals/arc 2052/Mark%20 Black well%20 Final%20 Report.htm as at 6th Jan. 2007.

[81] Meher, L.C., Sager, D.V., Naik, S.N., 2006. Technical aspects of biodiesel production by transesterification- a review. Renew. Sustain. Energy Rev. 10, 248–268.

[82] Meneghetti, S.M.P., Meneghetti, M.R, Wolf, C.R, Silva, E.C, Lima, G.E.S, De Lira Silva, L., Serra, T.M., Cauduro, F., & De Oliveira, L.G. (2006). Biodiesel from Castor Oil: A Comparison of Ethanolysis versus Methanolysis. *Energy and Fuels*, Vol. 20, No. 5, (September 2006), p.p. 2262-2265, ISSN 08870624.

[83] Mether, L.C. Dharmagadda, V.S.S. and Naik, S.N. (2006). Optimization of alkali-catalyzed transesterification of pongamia pinnata oil for production of biodiesel. *Bioresource Technology*, 97, 1392-1397.

[84] Miller-Klein Associates (2006).Use of Tallow in Biodiesel. Available at http://www.hgca.com/publications/document/use_of_tallow_in_biodie sel.pdf as at 26th Feb., 2009.

[85] Minami, E., Saka, S., 2006. Kinetics of hydrolysis and methyl esterification for biodiesel production in two-step supercritical methanol process. Fuel 85, 2479–

[86] Mittelbach, M. & Remschmidt, C. (Eds.) (2004).*Biodiesel: The Comprehensive Handbook*, Boersedruck Ges.m.b.H, ISBN 3-200-00249-2, Vienna, Austria

[87] Mittelbach, M. and Marr, R., 1995, "A low waste process for the production of biodiesel", Sep Science Technology, Vol. 30 (7-9), pp. 2021-2033.J. Van Gerpen, "Biodiesel processing and production," *Fuel Process. Technol.*, Vol. 86, no. 10, pp 1097-1107, 2005.

[88] Morgenstern, M.; Cline, J.; Meyer, S.; Cataldo, S. Determination of the kinetics of biodiesel production using proton nuclear magnetic resonance spectroscopy (1HNMR). *Energy Fuels* 20, 1350-1353 (2006).

[89] Mulimani, H.; Hebbal, O. D.; Navindgi, M. C. (2012)Extraction of Biodiesel from Vegetable Oils and Their Comparisons, *International Journal of Advanced Scientific Research and Technology*, 2(2), 242-250.

[90] Mythili, R. Venkatachalam, P. Subramaniam, P. and Uma, D. (2014). Production Characterization and Efficiency of Biodiesel: A Review. *International Journal of Energy Research*, John Wiley & Sons, Ltd.

[91] Nakatani, N. Takamori, H. Takeda, K. and Sakugawa, H. (2009).Transesterification of Soybean Oil Using Combusted Shell Waste as a Catalyst. *Bioresource Technology*, 100, 1510-1513.

[92] National Standards for Biodiesel (2009).A Sunday Energy Inc. Biodiesel, Minneapolis, Resource Document. Available at: http://bdresource.com/index.php?option=com_content&task=view&id=177&Itemid=30. As at July 14.

[93] Ngamcharussrivichai, C. Totarat, P. and Bunyakiat, K. (2008). Ca and Zn Mixed Oxide as a Heterogeneous Base Catalyst for Transesterification of Palm Kernel Oil. *Applied Catalysis A: General*, 341(1-2), 77-85.

[94] Ngamcharusssrivichai, C. Wiwatnimit, W. and Wangnoi, S. (2007).Modified Dolomites as Catalysts for Palm Kernel Oil Transesterification. *Journal of Molecular Catalysis: A Chemical*, 276, 24-33.

[95] Nijiu, S. Meera, S. Begun, K.S. and Anantharaman, N. (2014). Modification of Eggshell and its Application in Biodiesel Production. *Journal of Saudi Chemical Society*, 18, 702-706.

[96] Noordin, M. Y.; Venkatesh, V. C.; Sharif, S.; Elting, S.; Abdullah, A. Application of response surface methodology in describing the performance of coated carbide tools when turning AISI 1045 steel. *J. Mater. Proc. Technol.* 145, 46-58 (2004)

[97] O.D. and Yusuff, A.S. (2016). Synthesis of Biodiesel from Palm Kernel Oil Using Mixed Clay- Eggshell Heterogeneous Catalyst. *Iranica Journal of Energy and Environment*, 7(3) 308-314.

[98] Obadiah, A. Swaroopa, G.A. Kumar, S.V. Jeganathan, K.R. and Ramasubbu, A. (2012). Biodiesel Production from Palm Oil Using Calcined Waste Animal Bone as Catalyst. *Bioresource Technology*, 116, 512-516.

[99] Ofoefule Akuzuo Uwaoma , Esonye Chizoo , Onukwuli Okechukwu Dominic , Nwaeze Emmanuel , Cyril Sunday Ume. Modeling and optimization of African pear seed oil esterification and transesterification using artificial neural network and response surface methodology comparative analysis. Article in Industrial Crops and Products ·

August 2019 DOI: 10.1016/j.indcrop.2019.111707

[100] Ogbu, I.M.; Ajiwe, V.I.E. (2013) Biodiesel Production via Esterification of Free Fatty Acids from Cucurbita Pepo L.Seed Oil: Kinetic Studies. *International Journal of Scienceand Technology*, 2(8), 616-621.

[101] Olafedehan, O.A. (2010). Reaction Kinetics and Catalysis Note for Postgraduate Students.Department of Chemical Engineering, University of Lagos, Akoka Lagos Nigeria.

[102] Olusegun, H.D. and Ajiboye, T.K. (2009). Design Construction and Testing of Vibrator-Compactor Block Making Machine for Rural Application. *International Journal of Engineering*, 3(1), 1-14.

[103] Olutoye, M.A. and Hameed, B.H. (2013).A Highly Active Clay-Based Catalyst for the Synthesis of Fatty Acid Methyl Ester from Waste Cooking Palm Oil.*Applied Catalysis A: General*. 450, 57-62.

[104] Olutoye, M.A. Wong, S.W. Chin, L.H. Asif, M. and Hameed, B.H. (2015).Synthesis of Fatty Acid Methyl Esters via Transesterification of Waste Cooking Oil by Methanol with a Barium-Modified Montmorillonite K10 Catalyst.*Renewable Energy*, 86, 392-398.

[105] Parawira, W. (2010) Biodiesel production fromJatrophacurcas: A review.*Scientific Research and Essays*,5(14), 1796-1808.

[106] Park, Y.M. Chung, S.H. Eom, H.J. Lee, J.S. and Lee, K.Y. (2010).Tungsten Oxide Zirconia as Solid Superacid Catalyst for Esterification of Waste Acid Oil (Dark Oil).*Bioresource Technology*, 101 (17), 6589-6593.

[107] Patil PD, Gude VG, Mannarswamy A, Deng S, Cooke P, Munson-McGee S, Rhodes I, Lammers P, Nirmalakhandan N (2011) Optimization of direct conversion of wet algae to biodiesel under supercritical methanol conditions. Bioresource Tech 102, 118–22.

[108] Paton, T.R. Humphreys, G.S. and Mitchell, P.B. (1995).*Soils: A Global View*: London: UCL Press.

[109] Pazouki, M. Zamani, F. Zamzamcan, A.H. Fahar, M. and Najafpour, G. (2010).Esterification of Free Fatty Acids by Rhizopus Oryzae as Cell-Catalyzed from Used Cooking Oil for Biodiesel Production. *World Applied Sciences Journal*, 8(6), 719-724.

[110] Peña, R., Romero, R., Martínez S.L., Ramos, M.J., Martínez, A. & Natividad, R. (2009).Transesterification of Castor Oil: Effect of Catalyst and Co-Solvent. *Industrial and Engineering Chemistry Research*, Vol. 48, No. 3, (February 2009), p.p.1186–1189, ISSN 0888-5885

[111] Peng, B.X. Shu, Q. Wang, J.F. Wang, G.R., Wang, D.Z. and Han, M.H. (2008).Biodiesel Production from Waste Oil Feedstock by Solid Acid Catalysis.*Process Safety and Environmental Protection*, 86 (6), 441-447.

[112] Queda, N. Bonzi, Y.L. and Quedraogo, I.W.K. (2017). Deactivation, Process, Regeneration Conditions and Reusability Performance of CaO Or MgO Based Catalysts Used for Biodiesel Production- A Review. *Material Science and Applications*. 8, 94-122.

[113] Ragauskas, A.E. Yunqiao, P. and Ragauska, J. (2013).Biodiesel from Grease Interceptor to Gas Tank.*Energy Science and Engineering,* 1(1), 42-52.

[114] Raine RR, Johnson TR, Blackett B, Farid MM, Behzadi S, Elder ST(2008). New Zealand Tallow Sourced Biodiesel – A Review of theResource, Production and Engine Performance, U21 InternationalConference on Energy Technologies and Policy, Auckland, 8th-10thSept. pp. 1-15.

[115] Ramu, S. Lingaiah, N. Prabhavathi Devi, B.L.A. Prasad, R.B.N. Suryanarayana, I. and Sai Prasad, P.S. (2004). Esterification of Palmitic Acid with Methanol over Tungstenoxide Supported on Zirconia Solid Acid Catalysts: Effect of Method of Preparation of the Catalyst on its Structural Stability and Reactivity. *Applied Catalysis A: General*, 276 (1- 2), 163-168.

[116] Rao, T.V., Rao, G.P., Reddy, K.H.C. *Experimental Investigation of Pongamia, Jatropha and Neem Methyl Esters as Biodiesel on C.I. Engine*. Jordane Journal of Mechanical and Industrial Engineering vol. 2. 2: 117-122, 2008.

[117] Rashid U, Farooq A, Gerhard K (2009). Evaluation of biodiesel obtained from cottonseed oil. Fuel Process. Technol. 90(9): 1157-1163.

[118] Rojas, S. (2013) Preparation of Catalyst: Heterogeneous Catalyst. ICP-CSIC.

[119] Rutto, H. (2013). The Use of Thermally Modified Kaolin as a Heterogeneous Catalyst for Producing Biodiesel.*Material and Process for Energy: Communicating current research and Technological development*, 399-406.

[120] Ryan, T.W., Dogne, L.G. & Callahan, T.J. (1984). The effects of vetable oil properties on injection and combustion in two different diesel engines. *Journal of the American Oil Chemists' Society, Vol.* 61, No. 10, (October 1984), p.p. 1610-1619, ISSN 0003-021X

[121] Salamatinia B, Mootabadi H, Bhatia S, Abdullah AZ (2010) Optimization of ultrasonic-assisted heterogeneous biodiesel production from palm oil: A response surface methodology approach. Fuel Process Tech 91, 441–8.

[122] Santos, O.; Maruyama, S. A.; Claus, T.; Desouza, N. E.; Matsushita, M.; Visentainer, J. V. A novel response surface methodology optimization of base-catalyzed soybean oil methanolysis. *Fuel* 113, 580-585 (2013)

[123] Sengo I, Gominho J, d'Orey L, Martins M, d'Almeida- Duarte E, Pereira H, Ferreira-Dias S (2010) Response surface modeling and optimization of biodiesel production from Cynara cardunculus oil. Eur J Lipid Sci Tech 112, 310–20.

[124] Shah, B. Sulaimana, S. Jamal, P. and Alam, M.Z. (2014).Production of Heterogeneous Catalyst for Biodiesel Synthesis. *International Journal of Chemical and Environmental Engineering*, 5(2), 73-75.

[125] Sharma, V. and Sumbali, G. (2013).An Overview of the Symbiotic Interaction between Ants, Fungis and Other Living Organisms in Ant-Hill Soil.*International Journal of Environmental Science,* 4(3), 432-443.

[126] Sharma, Y.C. Singh, B. and Korstad, J. (2010).Application of an Efficient Nonconventional Heterogeneous Catalyst for Biodiesel Synthesis from *Pongamia Pinnata* Oil.*Energy Fuels*, 24, 3223-3231.

[127] Sirichai, C.A. Apanee, L. and Samai, J. (2012).Biodiesel Production from Palm Oil Using Heterogeneous Base Catalyst.*International Journal of Chemical and Biological Engineering,* 6, 230-235.

[128] Sivakumar, P.; Sindhanaiselvan, S.; Gandhi, N. N.; Devi, S. S.; Renganathan, S. Optimization and kinetic studies on biodiesel production from underutilized Ceiba Pentandra oil. *Fuel* 103, 693-698□2013□.

[129] Sivasamy, A. Cheah, K.Y. Fornasiero, P. Kemausuor, F. Zinoviev, S. and Miertus, S. (2009). Catalytic Applications in the Production of Biodiesel from Vegetable Oils. *ChemSusChem*, 2, 278-300.

[130] Soriano Jr. NU, Venditti R, Argyropoulus DS (2006). Biodiesel Synthesis via Homogeneous Lewis acid catalyzed transesterification. Fuel. 88(3): 560-565

[131] Stone, R.H. and Ndu, F.O.C. (1985).*New Biology for West African Schools*: New York, USA: Longmans Group Ltd.

[132] Sue, K. Kimura, K. Yamamoto, M. and Aras, K. (2004).Rapid Hydrothermal Synthesis of ZnO Nanorods without Organics.*Materials Letters*, 58(26), 3350-3352.

[133] Sulaiman, S. Khairudin, N. Jamah, P. Alam, M.Z. Zainudi, Z. and Azmi, S. (2014). Characterization of Fish Bone Catalyst for Biodiesel Production.*International Journal of Biological, Food, Veterinary and Agricultural Engineering*, 8(5), 464-466.

[134] Suppes, G.J., Dasari, M.A., Doskocil, E.J., Mankidy, P.J., Goff, M.J., 2004. Transesterification of soybean oil with zeolite and metal catalysts.Appl. Catal. A: Gen. 257, 213–223.

[135] Tan KT, Lee KT, Mohamed AR (2010) Optimization of supercritical dimethyl carbonate (SCDMC) technology for the production of biodiesel and value-added glycerol carbonate. Fuel 89, 3833–9.

[136] Tan, Y.H. Abdullah, M.O. Hipolito, C.N. and Taufiq-Yap., Y.H. (2015). Waste Ostrich and Chicken-Eggshells as Heterogeneous Base Catalyst for Biodiesel Production from Used Cooking Oil: Catalyst Characterization and Biodiesel Yield Performance. *Applied Energy*, 2, 1-13.

[137] Tashtoush GM, Al-Widyan MI, Al-Jarrah MM (2004) Experimental study on evaluation and optimization of conversion of waste animal fat into biodiesel. Energ Convers Manag 45, 2697–11.

[138] Taufiq-Yap, Y.H. Abdullah, N.F. and Basri, M. (2011).Biodiesel Production via Transesterification of Palm Oil Using NaOH/Al2O3 Catalysts.*Sains Malaysiana,* 40(6): 587-594.

[139] Teixeira, A.P.C. Santos, E.M. Vieira, A.F.P. and Lago, R.M. (2013) Use of Chrysotile to Produce Highly Dispersed K-doped MgO Catalyst for Biodiesel Synthesis.*Chemical Engineering Journal*, 232, 104-110.Olutoye, M.A. Adeniyi,

[140] Tyagi, S. O., Atray, N., Kumar, B., & Abhadatta, A. (2010). Journal of Metrology Society of India. Production, Characterization and

Development of Standards for Biodiesel - A Review, 197-218.

[141] Umdu, E.S. Tuncer, M. and Seker, E. (2009). Transesterification of *Nannochloroplasts aculata* microalga's lipid to biodiesel on Al2O3 supported CaO and MgO catalysts. *Bioresource Technology,* 100, 2828-2831.

[142] Van Gerpen JH, Peterson CL, Goering CE (2007). Biodiesel: AnAlternative Fuel for Compression Ignition Engines, Presented at the2007 Agricultural Equipment Technology Conference, Louisville, Kentucky, USA, 11-14th Feb., ASAE Publication Number 913C0107.

[143] Verziu M., Cojjocaru B., Hu J., Richards R., Ciuculescu C., & Filip P. (2008). Sunflower and rapeseed oil transesterification to biodiesel over different nanocrystalline MgOcatalysts. *Green Chemistry,* Vol. 10, No. 4, p.p.373-381, ISSN 1463-926

[144] Vicente, G., Martínez, M., & Aracil, J. (2004). Integrated biodiesel production: a comparisonof different homogeneous catalysts systems. *Biresource Technology*, Vol.92, No.3,(May 2004), pp. 297-305, ISSN 0960-8524

[145] Vujicic, D.J. Comic, D. Zarubica, A. Micic, R. and Boskovic, G. (2010).Kinetics of Biodiesel Synthesis from Sunflower Oil over CaO Heterogeneous Catalyst. *Fuel*, 89(8), 2054-2061.

[146] Wang, T.; Briggs, J. L. Rheological and thermal properties of soybean Oils with modified FA compositions. *J.Am. Chem. Soc.* 79, 831-836 (2002)

[147] Wei, Z. Xu, C. and Li, B. (2009).Application of Waste Eggshell as Low-Cost Solid Catalyst for Biodiesel Production. *Bioresource Technology*, 100, 2883–2885.

[148] Wen, L. Wang, Y. Lu, D. Hu, S. and Han, H. (2010).Preparation of KF/CaO Nanocatalyst and its Application in Biodiesel Production from Chinese Tallow Seed Oil.*Fuel*, 89 (9), 2267-2271.

[149] Wen, Z. Yu, X. Tu, S. T. Yan, J. and Dahlquist, E. (2010).Synthesis of Biodiesel from Vegetable Oil with Methanol Catalyzed by Li-Doped Magnesium Oxide Catalysts *Applied Energy,* 87(3), 743-748.

[150] Wörgetter M, Prank lH, Rathbauer J, Bacovsky D (2006). Local and Innovative Biodiesel, Final Report. Francisca Josephinum-Biomass Logistics and Technology. Wieselburg, pp. 32-33.

[151] Xie, W. & Li, H. (2006).Alumni-supported potassium iodide as a heterogeneous catalyst for biodiesel production from soybean oil.*Journal of Molecular Catalysis A: Chemical*,Vol. 255, No. 1-2, (August 2006), p.p. 1-9, ISSN 1381-1169

[152] Yan, S.L. Salley, S.O. and Simon Ng, K.Y. (2009a). Simultaneous Transesterification and Esterification of Unrefined or Waste Oils over ZnO-La2O Catalysts. *Applied Catalysts A: General*, 353(2), 203-212.

[153] Yang, Z. and Xie, W. (2007). Soybean Oil Transesterification over Zinc Oxide Modified with Alkali Earth Metals. *Fuel Processing Technology*, 88(6), 631-638.

[154] Yee, K.F. and Lee, K.T. (2008). Palm Oil as Feedstock for Biodiesel Production via Heterogeneous Transesterification: Optimization Study. *International Conference on Environment* (ICENV), 1-5.

[155] Yuan X, Liu J, Zeng G, Shi J, Tong J, Huang G(2008) Optimization of conversion of waste rapeseedoil with high FFA to biodiesel using response surfacemethodology. Renew Energ 33, 1678–84.